การสังเคราะห์แบบไฮโดรเทอร์มอลของม้วนนาโนไทเทเนตจากอนุภาคไทเทเนียขนาดไมครอน
โดยใช้โซนิเคชัน พรีทรีตเมนต์

นายนาวิน วิริยะเอี่ยมพิกุล

วิทยานิพนธ์นี้เป็นส่วนหนึ่งของการศึกษาตามหลักสูตรปริญญาวิศวกรรมศาสตรดุษฎีบัณฑิต
สาขาวิชาวิศวกรรมเคมี   ภาควิชาวิศวกรรมเคมี
คณะวิศวกรรมศาสตร์ จุฬาลงกรณ์มหาวิทยาลัย
ปีการศึกษา 2550

HYDROTHERMAL SYNTHESIS OF TITANATE NANOROLL FROM MICRON-SIZED
TITANIA POWDER USING SONICATION PRETREATMENT

Mr. Nawin Viriya-empikul

A Dissertation Submitted in Partial Fulfillment of the Requirements

for the Degree of Doctor of Engineering Program in Chemical Engineering

Department of Chemical Engineering

Faculty of Engineering

Chulalongkorn University

Academic year 2007

Thesis Title   HYDROTHERMAL SYNTHESIS OF TITANATE NANOROLL FROM MICRON-SIZED TITANIA POWDER USING SONICATION PRETREATMENT
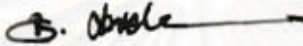
By   Mr. Nawin Viriya-empikul

Field of Study   Chemical Engineering

Thesis Advisor   Associate Professor Tawatchai Charinpanitkul, D.Eng.

Thesis Co-advisor   Professor Wiwut Tanthapanichakoon, Ph.D.

Accepted by the Faculty of Engineering, Chulalongkorn University in Partial Fulfillment of the Requirements for the Doctoral Degree

……………………………………………… Dean of Faculty of Engineering

(Associate Professor Boonsom Lerdhirunwong, Dr.Ing.)

THESIS COMMITTEE

…………………………………………Chairman

(Assistant Professor Varong Pavarajarn, Ph.D.)

……………………………………………Thesis Advisor

(Associate Professor Tawatchai Charinpanitkul, D.Eng.)

……………………………………… Thesis Co-advisor

(Professor Wiwut Tanthapanichakoon, Ph.D.)

……………………………………… External Member

(Chamorn Chawengkijwanich, Ph.D.)

………………………………………… Member

(Anongnat Somwangthanaroj, Ph.D.)

………………………………………… Member

(Apinan Soottitantawat, Ph.D.)

นาวิน วิริยะเอี่ยมพิกุล : การสังเคราะห์แบบไฮโครเทอร์มอลของม้วนนาโนไทเทเนตจากอนุภาคไท
เทเนียขนาดไมครอนโดยใช้โซนิเคชันพรีทรีตเมนต์. (HYDROTHERMAL SYNTHESIS OF
TITANATE NANOROLL FROM MICRON-SIZED TITANIA POWDER USING SONICATION
PRETREATMENT) อ. ที่ปรึกษา : รศ.ดร. ธวัชชัย ชรินพาณิชกุล, อ.ที่ปรึกษาร่วม : ศ. ดร. วิวัฒน์
ตัณฑะพานิชกุล จำนวนหน้า 65 หน้า.

ในการทำการศึกษาผลกระทบจาก ขนาดของสารตั้งต้นไทเทเนีย (400 นาโนเมตร และ 5 ไมโครเมตร) อุณหภูมิที่ใช้ใน
การสังเคราะห์ (90 ถึง 180 องศาเซลเซียส) และพลังงานที่ใช้ในการโซนิเคชัน (0 ถึง 38 วัตต์) พบว่าปัจจัยดังกล่าวสามารถ
ปรับเปลี่ยน รูปร่างของไทเทเนต ความยาวของท่อนาโนไทเทเนต และเฟสของไฟเบอร์นาโนไทเทเนตได้ โดยกล้องจุลทรรศน์
อิเล็กตรอนแบบส่องผ่าน (TEM) การดูดซับก๊าซไนโตรเจน (BET) เครื่องดีแอลเอส (DLS) และ เทคนิคการเลี้ยวเบนของรังสี
เอ็กซ์ (XRD) ได้ถูกนำมาใช้ในการวิเคราะห์ รูปร่าง พื้นที่ผิวจำเพาะ ขนาดเฉลี่ย และ เฟสของอนุภาคไทเทเนตที่สังเคราะห์ได้
โดยจากผลกระทบของขนาดของสารไทเทเนียตั้งต้น พบว่าอนุภาคของสารตั้งต้นที่มีขนาดเล็กกว่า จะสามารถเปลี่ยนเป็นไทเท
เนตที่มีรูปร่างระดับนาโนเมตรได้ง่ายกว่า รวมทั้งพื้นที่ผิวจำเพาะที่มากกว่าไทเทเนตที่สังเคราะห์จากสารตั้งต้นที่มีอนุภาคขนาด
ใหญ่กว่าด้วย สำหรับผลกระทบของอุณหภูมิ พบว่าเมื่ออุณหภูมิเพิ่มขึ้น ไทเทเนียที่มีรูปร่างทรงกลมจะเปลี่ยนรูปร่างไปเป็น แผ่น
ระดับนาโน ท่อระดับนาโน และ ไฟเบอร์ระดับนาโนตามลำดับ และลำดับของพื้นที่ผิวจำเพาะที่ได้รับผลกระทบเนื่องจาก
อุณหภูมิในการสังเคราะห์สามารถจัดลำดับได้ดังนี้ 150 > 120 > 90 > 180 องศาเซลเซียส ยิ่งไปกว่านั้นโซนิเคชันพรีทรีตเมนต์ก็
เป็นอีกปัจจัยหนึ่งที่ส่งผลกระทบต่อสมบัติของอนุภาคไทเทเนต เช่นกัน โดยเมื่อทำการใส่โซนิเคชันพรีทรีตเมนต์ ท่อนาโนไทเท
เนตที่ได้จะมีความยาว และพื้นที่ผิวจำเพาะที่เพิ่มมากขึ้น และยิ่งไปกว่านั้น เมื่อทำการเพิ่มพลังงานในการโซนิเคชันให้มากขึ้น (ที่
อุณหภูมิ 150 องศาเซลเซียส) พบว่าความยาวของท่อนาโนไทเทเนตก็เพิ่มขึ้นเช่นเดียวกัน อิทธิพลของโซนิเคชันพรีทรีตเมนต์
ไม่ได้มีผลเพียงแค่กับไทเทเนตที่มีรูปร่างแบบท่อ แต่ยังมีผลกับไฟเบอร์นาโนไทเทเนตอีกด้วย กล่าวคือ เมื่อทำการใส่ โซนิเค
ชันพรีทรีตเมนต์เข้าไปในการสังเคราะห์ไฟเบอร์นาโนไทเทเนตจะทำให้ไทเทเนตที่สังเคราะห์ได้มีเฟสบรุคไคท์ (เฟสหนึ่งของ
ไทเทเนต) เกิดขึ้นอีกด้วย

การแตกตัวของสารละลายฟีนอลถูกนำมาใช้ในการหาพฤติกรรมการเป็นตัวเร่งทางแสงของไทเทเนตที่สังเคราะห์ที่
อุณหภูมิ 90 ถึง 150 องศาเซลเซียส เมื่ออุณหภูมิที่เพิ่มขึ้นพื้นที่ผิวของไทเทเนตเพิ่มขึ้น (83-258 ตารางเมตรต่อกรัม) และ
แถบพลังงานช่องว่าง (จากเครื่อง UV/vis spectrometer) เพิ่มขึ้น (3.44-3.84 eV) แต่เนื่องจากการเปลี่ยนเฟสจากอะนาเทส ไปเป็น
เฟสของสารประกอบไทเทเนต ทำให้สาร ไทเทเนตที่สังเคราะห์ได้เกิดพฤติกรรมกันแสงยูวี แต่ไม่สามารถแสดงพฤติกรรมตัวเร่ง
ปฏิกิริยาทางแสงเพื่อแตกตัวฟีนอลได้

ภาควิชา.............วิศวกรรมเคมี................ ลายมือชื่อนิสิต........นาวิน วิริยะเอี่ยมพิกุล..........
สาขาวิชา.............วิศวกรรมเคมี................ ลายมือชื่ออาจารย์ที่ปรึกษา.........................
ปีการศึกษา 2550   ลายมือชื่ออาจารย์ทีปรึกษาร่วม.........................

4871813421   : MAJOR CHEMICAL ENGINEERING
KEY WORD: TITANATE NANOTUBE / HYDROTHERMAL PROCESS / SONICATION PRETREATMENT / PHOTOCATALYTIC / UV ADSORPTION

NAWIN VIRIYA-EMPIKUL : HYDROTHERMAL SYNTHESIS OF TITANATE NANOROLL FROM MICRON-SIZED TITANIA POWDER USING SONICATION PRETREATMENT. THESIS ADVISOR : ASSOC. PROF. TAWATCHAI CHARINPANITKUL, D.Eng., THESIS COADVISOR : PROF. WIWUT TANTHAPANICHAKOON, Ph.D., 65 pp.

Regarding to variation of size of TiO_2 powder (400 nm and 1 μm), reaction temperature (90-180 °C), and sonication power (0-38 W), morphology, length and phase of titanate nanostructures could be controlled. Transmission electron microscope (TEM), nitrogen adsorption (BET), dynamic light scattering (DLS) and X-ray diffractometer (XRD) have been employed to analyze structure, specific surface area, average size and crystalline phase of the synthesized products. For the effect of raw TiO_2 size, the smaller powder was transformed to titanate nanostructures with higher specific surface area than those of larger raw TiO_2 powder. Morphology of titanate product transformed from TiO_2 spherical particle to titanate nanosheet, nanotube and nanofiber with the gradual increase in the reaction temperature. The dependence of specific surface areas of titanate nanostructures on reaction temperatures are as follow: 150 > 120 > 90 > 180 °C. Based on the effect of sonication power, the length and BET surfacte area of titanate nanotube (TNT) becomes longer and larger, respectively, with the applying sonication pretreatment. Furthermore, at 150 °C, much longer TNTs with average hydrodynamic size of 490-1760 nm were produced when the sonication power was increased and the reported nanotube formation phenomena during the hydrothermal process, that is a mechanism contributing to length control is proposed. The interesting brookite phase was obtained after applying sonication pretreatment to synthesized titanate nanofiber.

The photocatalytic activity of titanate nanostructures synthesized by hydrothermal process at the reaction temperature of 90 °C to 150 °C was investigated by degradation of phenol solution in comparison with that of titania raw powder. With an increase in the hydrothermal reaction temperature (90-150°C), the specific surface area of titanate nanostructures became higher (83-258 m^2g^{-1}) and band gap energy (by UV/vis spectrometer) of titanate nanostructures also increased at 90-120 °C (3.44-3.84 eV) and slightly changed at 150°C (3.81 eV). Meanwhile, their phase changed from anatase to titanate compounds. Interestingly, the synthesized titanate exhibits high UV adsorption capability but no intrinsic photocatalytic activity for phenol degradation.

Department......Chemical Engineering........ Student's signature...Nawin Viriya-empikul.........

Field of study...Chemical Engineering........ Advisor's signature........T. Charoenpanithul....

Academic year .....2007............. Co-advisor's signature...W. Tanthapanichakoon..

ACKNOWLEDGEMENTS

CONTENTS

LIST OF TABLES

LIST OF FIGURES

Page

CHAPTER I

INTRODUCTION

1.1 Background

With novel properties and various potential applications, titanium dioxide (TiO_2) has obtained intensive attention for more than several decades. Although there are several kinds of photocatalysts such as TiO_2, ZnO, CdS, and $ZrTiO_4$, TiO_2 has considerable advantaged not only in its superior photocatalytic properties but also in its good characteristics of chemical stability, endurance, thin film transparency and so on. Many studies have been investigating its applications as a photocatalyst for water purification, and decomposition of harmful gases and organic compounds (Tanaka et al., 1999; Ao and Lee, 2005; Lachheb et al., 2002).

There are many researchers interested to increase the surface area by synthesizing to TiO_2 nanostructures. There are two major methods to fabricate TiO_2 nanotube, template replication and hydrothermal methods. By using template replication method (Gopal et al., 2005; Imai et al., 1999), well aligned and uniform TiO_2 nanotubes were obtained. However, the tube size obtained from this method was considerably large with diameters larger than 50 nm and difficult to separate the tubes from the template materials. On the other hand, the hydrothermal technique which converts TiO_2 powders to titanate nanotubes (TNTs) in alkali solution has been focused to provide remarkably high yield of TNTs. The TNTs have received increasing attentions with intension to control morphological configurations. This is attributable to the fact that TNTs could exhibit high specific surface area and new physical properties enable ion exchange and gas storage applications (Lim et al., 2005; Sun and Li, 2003).

Regarding the hydrothermal technique, it has been reported that there are many parameters including reaction temperature, concentration of NaOH and size of raw TiO_2 powders effecting the structure and characteristic of synthesized TNTs (Kasuge et al., 1998, 1999; Ma et al., 2005; Ma et al., 2006; Seo et al., 2001; Weng et al., 2006; Yuan et al., 2004). However, the knowledge to control the nanostructure (tubes and/or rods), equivalent size, diameter, and specific surface area have not clearly reported. In this work, the effects to synthesize titanate nanomaterials; the

micron sized TiO_2, reaction temperature, power of sonication pretreatment, will be investigated and discussed.

1.2 Objectives of Research Work

1.2.1 To hydrothermally synthesize titanate nanoroll from micron-sized TiO_2 powder using sonication pretreatment.

1.2.2 To investigate effect of synthesis conditions on the morphology, size, and specific surface area of titanate nanoroll.

1.3 Scopes of Research Work

1.3.1 Characterization of the raw TiO_2 material and obtained nanostructures:

a) Specific surface area and pore size distribution.

b) Approximate diameter and shape.

c) Particle size distribution (equivalent size).

d) Phase of structures.

1.3.2 Synthesis of titanate nanomaterial by hydrothermal method:

a) The average particle sizes of raw TiO_2 powders fall in the range 0.4-45 micrometer.

b) Ranges of reaction temperature are 90-180 ^{o}C.

c) Powers of sonication pretreatment are varied from 0 to 38 Watt.

1.4 Expected Benefits from This Work

1.4.1 The knowledge to control the nanostructure (tubes and/or rods) equivalent size, diameter, and specific surface area under the effect of micron size of raw material, reaction temperature, and power of sonication pretreatment will be obtained.

1.4.2 The production cost of titanate nanotube will be decreased by using cheaper raw TiO_2 materials in micron size.

CHAPTER II

FUNDAMENTAL KNOWLEDGE AND LITERATURE REVIEW

2.1 Typical methods to prepare nanostructures of titanate and TiO_2

Recently, there are two major methods, template assisted and alkaline hydrothermal, to improve the properties of TiO_2, such as specific surface area, photocatalytic activity, and so on. However, the method to synthesize nanostructure material should be considered because these two synthesis methods have the advantage and disadvantage.

2.1.1 Template assisted
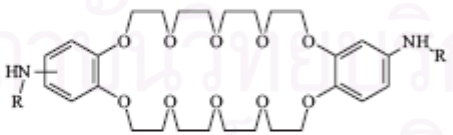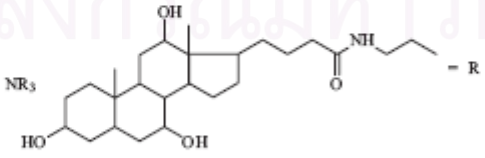
The template synthesis method is focused by several scientists because it is very general; by controlling the shape of template, the nanomaterial or micromaterial is obtained. Dmitry et al. (2006) summarized the diameter of TiO_2 nanotube depended on the condition of self-assembled organic surfactant template molecules as shown in table 2.1. From table 2.1, the wildly nanotube diameter is shown. It means that the controlling of tube diameter was obtained by changing the organic surfactant template. However, the template assisted method has disadvantage being difficult to separate the tubular product from the template materials.

2.1.2 Alkaline hydrothermal

Alkaline hydrothermal method has been firstly reported by Kasuga et al. (1998). They synthesized TiO_2 nanotube (titanate nanotube) by reacting TiO_2 (anatase phase) with NaOH aqueous solution. Because of its simple method and high yield of slender titanate nanotube (diameter <10 nm), after reporting of Kasuga et al. (1998, 1999), the research about titanate nanostructure synthesized by hydrothermal method has been focus with much interest such as chemical formula (Yang et al., 2003; Ma et al., 2005; Thorne et al., 2005), physical properties (Yang et al., 2003; Du et al., 2001; Kim et al., 2006; Ma et al., 2005; Qian et al., 2005; Seo et al., 2001; Sun and Li,

2003; Thorne et al., 2005) and potential application (Kim et al., 2006; Sun and Li, 2003; Oh and Jin, 2006; Xu et al., 2005; Idakiev et al., 2005). Moreover, the several parameters, including reaction temperature, concentration of NaOH and size of raw TiO_2 powder, jointly determine the structure and characteristics of synthesized TNTs, have been reported (Kasuga et al., 1998; 1999; Ma et al., 2005; 2006; Seo et al., 2001; Weng et al., 2006; Poudel et al., 2005; Yuan and Su, 2004). Nevertheless, a disadvantage of hydrothermal method has been investigated. Since, after hydrothermal reaction, titanate nanostructure could not show the photocatalytic activity (as discuss in Chapter 5), the post-treatment, calcination or removing of Na ion, has been considered to improve its activity.

Table 2.1 Morphological properties of TiO_2 nanotubes produced by the sol–gel method in the presence of templating agents. Bu=n-butyl; iPr=isopropyl. (Dmitry et al., 2006)

Precursor	Template	Conditions	Nanotube diameter [nm]
Ti(OiPr)$_4$		25 °C, ethanol, NH$_4$OH	50–300
Ti(OiPr)$_4$		25 °C, 1-butanol, benzylamine	500
Ti(OBu)$_4$		25 °C, ethanol, CH$_3$COOH, H$_2$O	4–7
Ti(OBu)$_4$	CH$_3$(CH$_2$)$_{11}$NH$_2$·HCl	25–40 °C, H$_2$O	1800–6000
Ti(OiPr)$_4$	Tobacco mosaic viruses	25 °C, ethanol	20
Ti(OBu)$_4$	[Pt(NH$_3$)$_4$](HCO$_3$)$_2$	25 °C, ethanol	100
Ti(OiPr)$_4$	Porous alumina	25 °C, pressure impregnation	60–70
TiF$_4$	Porous alumina	60 °C, HCl	2.5–5, 70–100
Ti(OiPr)$_4$	Porous alumina	25 °C, ethanol, CH$_3$COOH	120–140

2.2 Titanium dioxide photocatalyst

Starting in the late 1960s, Fujishima et al. have been involved in an unfolding story whose main character is the fascinating material titanium dioxide (TiO_2). This story began with photoelectrochemical solar energy conversion and then shifted into the area of environmental photocatalysis, including self-cleaning surfaces, and most recently into the area of photoinduced hydrophilicity, which involves not only self-cleaning surfaces, but also antifogging ones. One of the most interesting aspects of TiO_2 is that the types of photochemistry responsible for photocatalysis and hydrophilicity are completely different, even though both can occur simultaneously on the same surface.

Titania is commercially very important as a white pigment because of its maximum light scattering with virtually no absorption and because it is non toxic, chemically inert, and a dielectric ceramic material for its higher dielectric constant (Cheng et al., 1995). Recently, it has been suggested that monodisperse oxide powders are preferable to ceramic raw materials (Ogihara et al., 1991). Titania is known to have several natural polymorphs: Rutile is thermodynamically stable which tends to be more stable at high temperatures and thus is sometimes found in igneous rocks, but anatase is metastable at high temperatures (both belonging to the tetragonal crystal system), and bookite is found only under hydrothermal conditions or usually found only in minerals and has a structure belonging to the orthorhombic crystal system (Keesmann, 1966). Anatase type titania has been used as a catalyst for photodecomposition and solar energy conversion, because of its high photoactivity (Fox and Dulay, 1993; Fujishima et al., 2000). On the other hand, rutile-type titania has been use for white pigment materials, because of its good scattering effect, which protects materials from ultraviolet light. Anatase titania has been reported to be unstable at high temperature and its transformation temperatures to be scattered in a wide range. Polymorphic transformation of ceramic materials generally depends on the grain size, impurities, composition, nature of the dopant, amount of dopant, and processing (Hirano et al., 2002).

2.2.1 Properties of titanium dioxide

Titanium (atomic number 22; ionization potentials: first 6.83 eV, second 13.67 eV, third 27.47 eV, fourth 43.24 eV) is the first member of Group IVB of the periodic chart. It has four valence electrons, and Ti (IV) is most stable valence state. The lower valence state Ti (II) and Ti (III) exist, but these are readily oxidized to the tetravalent state by air, water, and other oxidizing agent. The ionization potentials indicate that the Ti^{4++} ion would not be expected to exist and, indeed, Ti (IV) compounds are generally covalent. Titanium is able to expend its outer group of electrons and can form a large number of addition compounds by coordination other substances having donor atom, e.g., oxygen or sulfur. The most important commercial forms are titanium (IV) oxide and titanium metal.

Titanium (IV) oxide occurs naturally in three crystalline form: anatase, which tends to be more stable at low temperature, brookite, which is usually found only in materials, and rutile, which tends to be more stable at higher temperatures and thus is sometimes found in igneous rock. These crystals are substantially pure titanium (IV) oxide but usually amounts of impurities, e.g., iron, chromium, which darken them. A summary of three varieties is given in Table 2.2.

Although anatase and rutile are both tetragonal, they are not isomorphous (fig. 2.2). Anatase occurs usually in near-regular octahedral, and rutile forms slender prismatic crystal, which are frequently twinned. Rutile is the thermally stable form and is one of the two most important ores of titanium.

The three alltropic forms of titanium (IV) oxide have been prepared artificial but only rutile, the thermally stable form, has been obtained in the form of transparent large single crystal. The transformation form anatase to rutile is accompanied by the evolution of ca. 12.6 kJ/mol (3.01 kcal/mol), but the rate of transformation is greatly affected by temperature and by the presence of other substance which may either catalyze or inhibit the reaction. The lowest temperature at which conversion of anatase to rutile takes place at a measurable rate is ca. 700 ^{o}C, but this is not a transition temperature. The change is not reversible; ΔG for the change from anatase to rutile is always negative.

Brookite has been produced by heating amorphous titanium (IV) oxide, prepared from an alkyl titanates of sodium titanate with sodium or potassium

hydroxide in an autoclave at 200 to 600 ^{o}C for several day. The important commercial forms of titanium (IV) oxide are anatase and rutile, and these can readily be distinguished by X-ray diffraction spectrometry.

Since both anatase and rutile are tetragonal, they are both anisotropic, and their physical properties, e.g. refractive index, very according to the direction relative to the crystal axes. In most applications of these substances, the distinction between crystallographic direction is lost because of the random orientation of large numbers of small particles, and it is mean value of the property that is significant.

Table 2.2 Crystallographic properties of rutile, anatase, and brookite. (Ulrike, 2003)

Crystal structure	System	Space group	Lattice constants (nm)			
			a	b	c	c/a
rutile	Tetragonal	D$_{4h}^{14}$-P4$_2$/mnm	0.4584	–	0.2953	0.644
anatase	Tetragonal	D$_{4h}^{19}$-I4$_1$/amd	0.3733	–	0.937	2.51
brookite	Rhombohedral	D$_{2h}^{15}$-Pbca	0.5436	0.9166	0.5135	0.944

Density (kg/m^3)	
rutile	4240
anatase	3830
brookite	4170
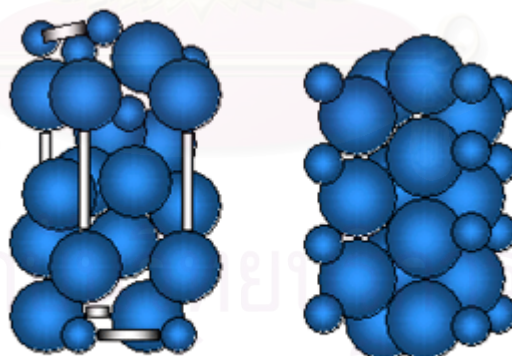
Fig. 2.1. Crystal structure of TiO$_2$. (Fujishima et al., 2000)

2.2.2 Principles of photocatalytic reaction (Hoffmann et al., 1995)

Semiconductor photocatalysis with a primary focus on TiO_2 as a durable photocatalyst has been applied to a variety of problems of environmental interest in addition to water and air purification. It has been shown to be useful for the destruction of microganisms such as bacteria (Ireland et al., 1993) and viruses (Sjogren et al., 1994), for the inactivation of cancer cells, (Cai et al., 1992) for odor control (Suzuki, 1993), for the photosplitting of water to produce hydrogen gas, (Karakitsou and Verykios, 1993; Gratzel, 1981; Borgarello et al., 1981; Duonghong et al., 1981; Kalyanasundaram et al., 1981) for the fixation of nitrogen, (Khan et al., 1992; Schiavello, 1993) and for the clean up of oil spills (Gerischer and Heller, 1992; Jackson et al., 1991).

Semiconductors (e.g., TiO_2, ZnO, Fe_2O_3, CdS, and ZnS) can act as sensitizers for light-reduced redox processes due to their electronic structure, which is characterized by a filled valence band and an empty conduction band (Nair et al., 1993). When a photon with an energy of hv matches or exceeds the bandgap energy, E_g, of the semiconductor, an electron, e_{cb}^-, is promoted from the valence band, VB, into the conduction band, CB, leaving a hole, h_{vb}^+ behind (see Fig. 2.3). Excited state conduction-band electrons and valence-band holes can recombine and dissipate the input energy as heat, get trapped in metastable surface states, or react with electron donors and electron acceptors adsorbed on the semiconductor surface or within the surrounding electrical double layer of the charged particles.

In the absence of suitable electron and hole scavengers, the stored energy is dissipated within a few nanoseconds by recombination (Boer, 1990). If a suitable scavenger or surface defect state is available to trap the electron or hole, recombination is prevented and subsequent redox reactions may occur. The valence-band holes are powerful oxidants (+1.0 to +3.5 V vs normal hydrogen electrode (NHE) depending on the semiconductor and pH), while the conduction-band electrons are good reductants (+0.5 to -1.5 V vs NHE). Most organic photodegradation reactions utilize the oxidizing power of the holes either directly or indirectly; however, to prevent a buildup of charge one must also provide a reducible species to react with the electrons. In contrast, on bulk semiconductor electrodes only one species, either the hole or electron, is available for reaction due to band bending

(Rothenberger et al., 1985). However, in very small semiconductor particle suspensions both species are present on the surface. Therefore, careful consideration of both the oxidative and the reductive paths is required.
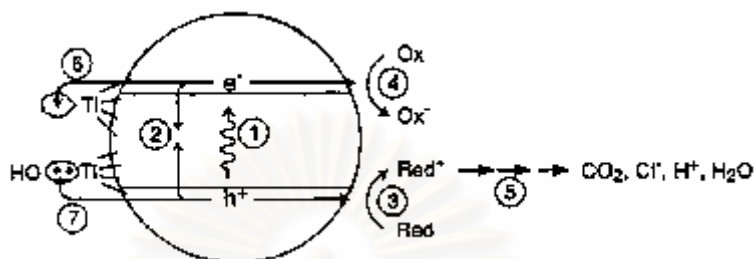
Fig. 2.2. Primary steps in the photoelectrochemical mechanism: (1) formation of charge carriers by a photon; (2) charge carrier recombination to liberate heat; (3) initiation of an oxidative pathway by a valence-band hole; (4) initiation of a reductive pathway by a conduction-band electron; (5) further thermal (e.g., hydrolysis or reaction with active oxygen species) and photocatalytic reactions to yield mineralization products; (6) trapping of a conduction-band electron in a dangling surficial bond to yield Ti(III); (7) trapping of a valence-band hole at a surficial titanol group.

2.3 Potential applications of titanate nanostructure

Since the changing of chemical formula and increasing of specific surface area, several researches try to find out the new application of titanate nanostructure such as bone growth, dye-sensitized solar cell and supported material.

Oh and Jin (2006) treated the surface of TiO_2 array with NaOH solution. TiO_2 surface was transformed to sodium titanate which suitable for growth the osteoblast cells. Moreover, the number of the adhered cells on the TiO_2 nanotubes increases by as much ca. 400% as compared to the Ti metal.

Kim et al. (2006) fabricated the dye-sensitized solar cell composed with titanate nanotube. Two methods, electrophoretic deposition (EPD) and doctor-blade method, were employed to coat titanate nanotube film on the FTO (F-SnO_2 coated glass) substrates. The solar cell corresponding to electrodeposited titanate nanotubes annealed at 500 ^{o}C showed the efficiency at 6.71% while the solar cell fabricated with doctor-blade method using titanate nanotubes, annealed at 450 ^{o}C shows much lower efficiency at 0.65%, due to non-conversion of titanate nanotubes to titania, intercalated sodium and poor interfacial adhesion between titanate nanotubes and FTO substrate.

Xu et al. (2005) synthesized Zn ions surface-doped TiO_2 nanotubes. The Zn ions surface-doped TiO_2 nanotubes calcined at above 400 ^{o}C exhibit a further improvement on the photocatalytic activity for the degradation of methyl orange in water.

CHAPTER III

INVESTIGATION FOR LENGTH CONTROL OF TITANATE
NANOTUBES USING HYDROTHERMAL REACTION
WITH SONICATION PRETREATMENT

3.1 Introduction

With novel properties and various potential applications, titanium dioxide (TiO_2) has gained wide attention for decades. Among the semiconductor-type photocatalysts such as TiO_2, ZnO, and CdS (Fujishima et al., 2000; Diebold, 2003; Liu et al., 2006; Tseng et al., 2006; Daneshvar et al., 2004; Chakrabarti and Dutta, 2004; Rohe et al., 2006; Liu et al., 1998; Janet and Viswanath, 2006), TiO_2 commands several advantages including superior photocatalytic properties, excellent chemical stability, endurance, transparency and so on. Numerous studies have explored its applications as photocatalyst for water purification, decomposition of harmful gaseous organic compounds, and so on   (Ao and Lee, 2005; Lachheb et al., 2002; Tanaka et al., 1999; Kanki et al., 2005).

Recently control of morphological configurations of titanate nanotubes (TNTs) has received growing attention. This is attributable to the fact that TNTs could exhibit morphology and high specific surface areas necessary for ion exchange and gas storage applications (Lim et al., 2005; Sun and Li, 2003). Template replication and hydrothermal techniques are two major methods for fabricating TiO_2 nanotubes. In the template replication method (Imai et al., 1999; Gopal et al., 2005), well aligned and uniform TiO_2 nanotubes could be obtained. Nevertheless, such method is mostly suitable for making large nanotubes with diameters larger than 50 nm. Moreover, it is

difficult to separate the tubular product from the template materials (Dmitry et al., 2006). Here the hydrothermal technique, which converts TiO_2 powder to TNTs in alkali solution, was focused upon because it provided remarkably high yield of TNTs with small diameters (ca. 10nm).

Regarding the hydrothermal technique, it has been reported that several parameters, including reaction temperature, concentration of NaOH and size of raw TiO_2 powder, jointly determine the structure and characteristics of synthesized TNTs (Kasuga et al., 1998; 1999; Ma et al., 2005; Ma et al. 2006; Seo et al., 2001; Weng et al., 2006; Poudel et al., 2005; Yuan and Su, 2004). Recently, Ma et al. (2006) reported that, when the sonication time was longer than 60 min and power of sonication pretreatment was higher than 380 W, the morphology of synthesized product changed from nanosheets, which were peeled out of swelled TiO_2 surface, to become TNTs with various nominal lengths of c.a. 100-600 nm. In fact, the present authors have discovered that sonication pretreatment was not necessary for the synthesis of TNTs provided that a sufficiently long reaction time (1 day or longer) be used in the hydrothermal synthesis, and to the best of our knowledge, no investigation on synthesizing parameters that aims to control the average length of TNTs in the hydrothermal step has been reported. In this article, the authors report a practical simple step toward the length control of TNTs by low-power sonication pretreatment of TiO_2 powders in NaOH solution and delineate the role of this pretreatment on the subsequent formation of TNT.

3.2 Experimental

Commercial titania powder (KISHIDA, mean particle size = 400 nm, specific surface area claimed by company = 16 m^2g^{-1} and measured by this research = 8 m^2g^{-1}) was used as precursor to fabricate titanate nanotubes (TNTs) in a hydrothermal process. 0.5 g of the TiO_2 precursor with 50 ml of 10-M NaOH aqueous solution in a Teflon vessel was sonicated for 8 minutes using a titanium horn. Calibrated against the rate of temperature elevation of water in a thermally insulated vessel, the actual sonication power supplied to the solution was controlled in a range of 0 (no sonication) to 38.1 W. The sonicated suspension was poured into a Teflon vessel and placed in a hermetically sealed autoclave for hydrothermal treatment at 150°C for 3 days. Then the suspension was filtrated and treated with 0.1 M HCl solution. Finally, the synthesized particles were repeatedly washed with distilled water until the pH of the washing water reached 7, and then the particles were dried at 70°C in an oven. The synthesized products were characterized with a transmission electron microscope (TEM; JEOL, JIM2010), a particle size analyzer based on dynamic light scattering (DLS; Malvern Instruments, Zetasizer 3000HSA), an X-ray diffractometer (XRD; Rigaku, RINT 2000), and a surface area analyzer based on nitrogen adsorption (BEL, BelSorp-Mini II).

3.3   Results and discussion

We discovered that the average length and length distribution of the synthesized TNTs were significantly affected by the sonication pretreatment. More specifically, the average length of the TNTs was very short when the sonication pretreatment was not applied, but much longer TNTs were produced with this simple pretreatment. The next objective was to control the average length by adjusting the sonication power and reaction conditions.

Figure 3.1 exhibits the TEM images of the short TNTs. Their inner diameters were around 4-6 nm with multi-layered walls of 2 - 6 layers and interlayer spacing of ca. 0.8 nm. The lengths of these short TNTs ranged from 30 to 200 nm. In contrast, figures 3.2a and 3.2b exhibit the entangling long TNTs obtained with the use of sonication pretreatment at 7.6 and 38.1 Watts, respectively. Obviously these TNTs were much longer than the TNTs prepared without sonication pretreatment. The majority of these long TNTs exceeded 300 nm in length. Nevertheless, their inner diameter, number of wall layers and interlayer spacing were similar to those of the short TNTs. These key characteristics were checked and confirmed with repeatable XRD analyses.

Suzuki and Yoshikawa (2004) investigated d-spacing between adjacent tube layers of TNTs synthesized by the hydrothermal method at 110 $^{\circ}$C for 72 h in 10 M NaOH solution (TiO$_2$ 150 mg: NaOH solution 50 ml). HT-XRD (High Temperature X-Ray Diffraction) was employed to study the peak pattern of TNTs. As the TNTs were heated from room temperature to 200 $^{\circ}$C, the peak pattern was shifted from 2θ = 9.2° (0.92 nm) to 2θ = 11.2° (0.79 nm). The changing of d-spacing between adjacent layers occurred because water molecules were removed from the interlayer of the

TNT. Based on the XRD analyses of Suzuki and Yoshikawa, the deviation of the peak pattern around $2\theta = 10^{o}$ could be used to calculate the d-spacing of the present TNTs. In figure 3.3, XRD analyses of the samples prepared without (short TNTs) and with 7.6 and 38.1 W sonication pretreatment (long TNTs) exhibit a characteristic peak around $2\theta = 10^{o}$. These XRD analyses revealed that the interlayer spacing was not significantly affected by the sonication pretreatment. Importantly, it should be noted that the anatase peaks, which were found in the raw material, were not detectable in all synthesized TNT samples.

The results of DLS analyses shown in figure 3.4 revealed the particle size distributions (PSD) of the raw material and the TNTs fabricated with sonication power of 0, 7.6, and 38.1 Watts, respectively. Obviously the titania precursor exhibited a relatively broad size distribution. Interestingly, it was found that short TNTs with a remarkably narrow size distribution were produced without sonication pretreatment whereas both cases of long TNTs had a broader size distribution. More specifically, the DLS analyses showed that the average size of the TiO_2 powder is ca. 448 nm whereas the average sizes of TNTs prepared with sonication power of 0, 7.6 and 38.1 Watts were 53, 490 and 1760 nm, respectively. The huge difference in the average sizes of TNTs fabricated with and without sonication pretreatment could be attributed to distinct difference in the sizes of the nanosheets peeled from the surface of the swollen TiO_2 particles. Without the pretreatment, the average length of the short TNTs was an order of magnitude smaller than that of the raw material. However, with a low sonication power of 7.6 and 38.1 Watts the average size of the synthesized TNTs became larger than that of the titania precursor. It may be postulated from the formation mechanism of TNTs mentioned below that raw TiO_2 powder with a narrower PSD would yield a more nearly uniform size of nanosheets,

which represent the intermediate for the fabrication of TNTs. Further investigation to verify this postulate is being explored by the authors.

The results of Brunauer, Emmett and Teller (BET) specific surface area measurements with nitrogen adsorption are listed in table 3.1. As expected, all TNT samples showed significantly higher BET areas than that of the non-porous precursor particles because the TNTs were hollow and non-spherical. From theoretical estimation, the specific surface area of short and long TNTs should not differ significantly. However, table 3.1 reveals that the sonication pretreatment led to not only longer TNTs but also larger BET specific surface areas. It could be considered that the effect of sonication resulted in significantly higher overall reaction rate and yield of TNTs, thereby increasing the specific surface areas of the pretreated samples. In fact, the BET areas and average nominal lengths of the long TNT samples were ca. 1.4 and 8-9 times those of the short ones. This implies that the samples obtained with sonication pretreatment contained a significantly lower number of TNTs than that without pretreatment.

In general, the hydrothermal reaction between TiO_2 particles and NaOH solution started when the reactive Na^+ and OH^- species diffused to and began to digest the surface of TiO_2 particles, thereby causing the surface of the particles to swell and subsequently peel off as titanate nanosheets. Yang et al. (2003) showed TEM images of the swelling of a TiO_2 nanoparticle and a titanate nanosheet peeling off a swollen TiO_2 particle. The subsequent rolling of the nanosheets into nanotubes was also confirmed with TEM images (Yuan and Su, 2004; Du et al., 2001; Wang et al., 2002; Thorne et al., 2005; Dmitry et al., 2004) and separately via simulation (Wang et al., 2002; Zhang et al., 2003). In figure 5, the present authors proposed and illustrated schematically the effect of sonication pretreatment on the formation of TNTs.

Without sonication pretreatment, the precursor TiO_2 particles remained agglomerated. On the other hand, the sonicated precursor solution consisted of deagglomerated particles. When a solution was prepared without sonication, the initially suspended TiO_2 powder in the highly viscous NaOH solution rapidly settled down on the bottom of the vessel, even though stirring was applied. The phenomenon may be attributed to the agglomeration of the TiO_2 powder. However, with sonication pretreatment, the suspension changed to a milky-like liquid considered to consist of deagglomerated TiO_2 particles. In the case of non-sonicated precursor, the reactive Na^+ and OH^- species suffered retarded non-uniform local reaction rates because they could not freely penetrate into the narrow constricted inter-particle zones and could not thoroughly react with the entire TiO_2 surfaces. The disrupted non-uniform peeling of the swollen skins yielded small titanate nanosheets, including partially torn nanosheets. The small nanosheets could be rolled up to form only short TNTs. In short, the overall formation rate was controlled by diffusion or mass transfer rate. On the other hand, in the case of the sonicated suspensions, the reaction of NaOH on the surfaces of the deagglomerated TiO_2 particles was much more thorough and uniform, and so was the smooth unhindered peeling of the swollen skins, thereby resulting in large nanosheets, which were subsequently rolled into long TNTs.

Figure 3.6 clearly shows some experimental evidence of short TNTs formed without sonication pretreatment at reaction times of 1 day (figure 3.6a) and 3 days (figures 3.6b and 3.6c). After TiO_2 powder reacted with the NaOH solution for 1 day, small titanate nanosheets were obtained. Some of the nanosheets were rolled into short hollow titanate nanotubes. In figure 3.6b, by the end of the 3rd day some of the short TNTs were seen to separate from a bundle of the rolled nanosheets. Figure 6c gives a typical evidence of partially torn TNTs produced when two of the short TNTs

remained connected due to imperfect tearing of a nanosheet. In fact, partially torn
TNTs could also be observed in figures 3.1a and 3.6b.

Table 3.1 BET surface area of titanate nanotube as a function of power of sonication
pretreatment

Power of sonication (Watts)	0	7.6	38.1
BET surface area $(m^2g^{-1})^a$	179	258	245

^{a}TiO$_2$ raw powder = 8 m^2g^{-1}
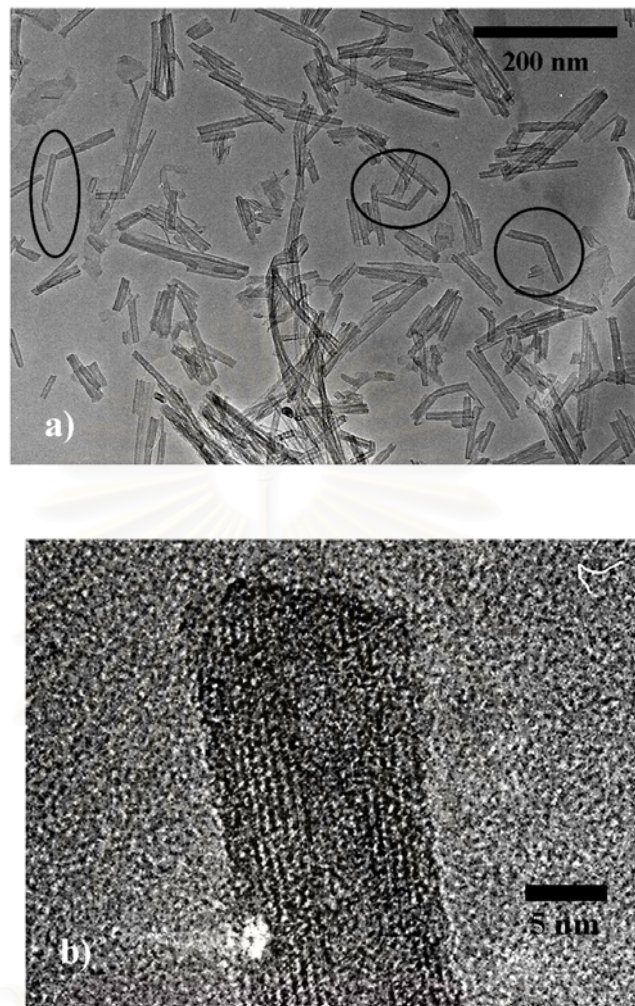
Figure 3.1 TEM image of the short titanate nanotubes obtained without sonication
pretreatment: a) low magnification image (the partially torn TNTs
marked by cycle); b) high magnification image.
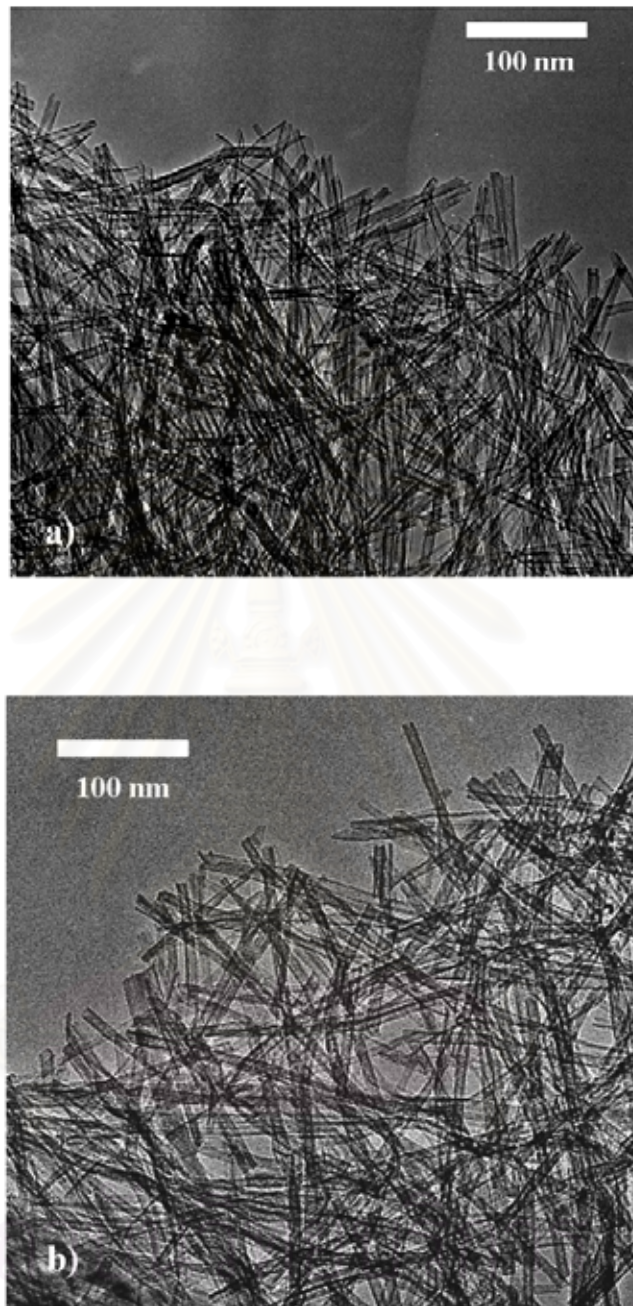
Figure 3.2 TEM image of the long titanate nanotubes obtained with a sonicated pretreatment power at a) 7.6 and b) 38.1 W.
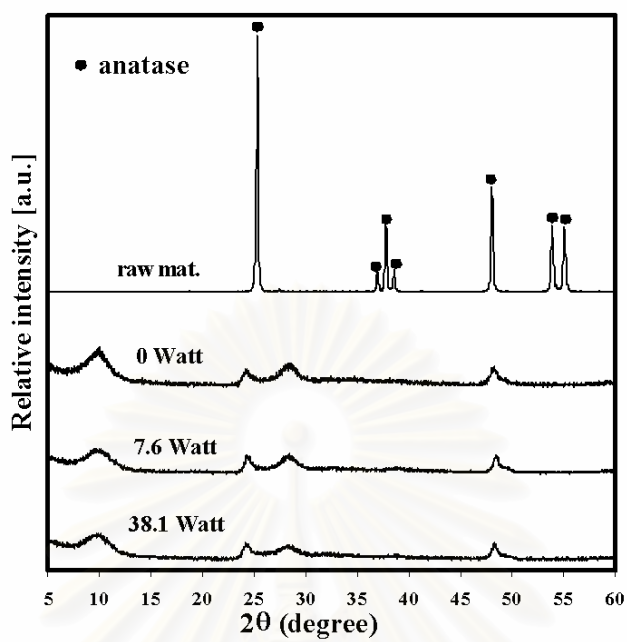
Figure 3.3   XRD spectra of raw TiO$_2$ powder, TNTs prepared with sonication

pretreatment at 0, 7.6, and 38.1 W.
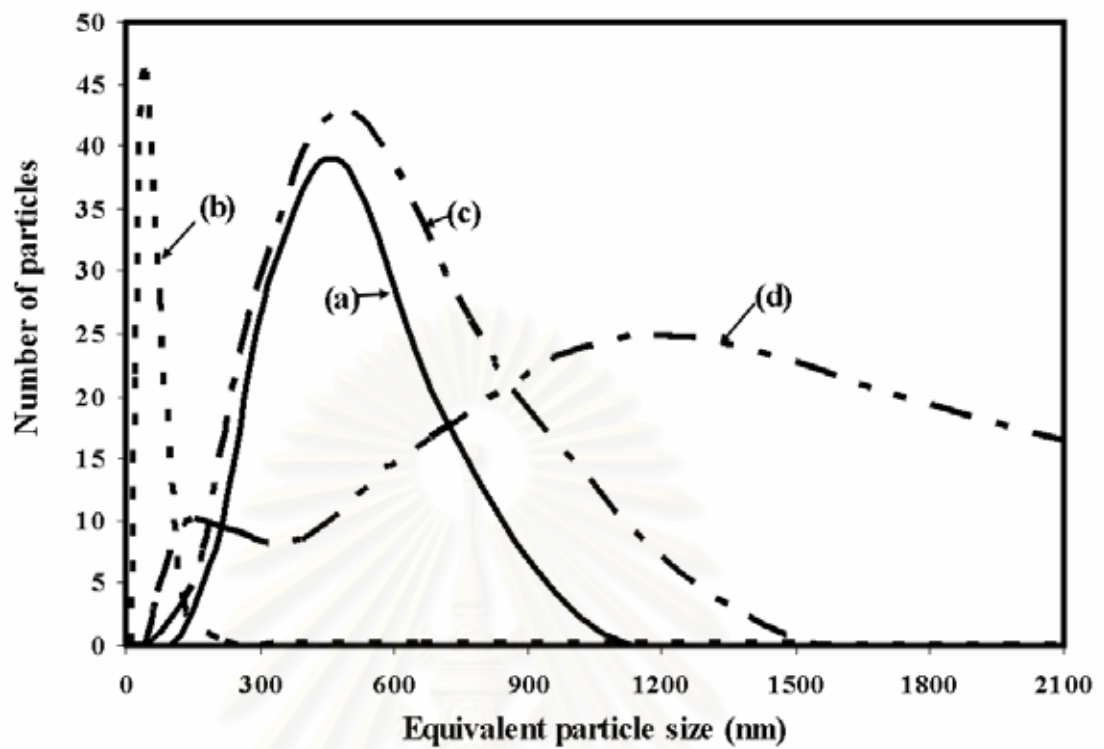
Figure 3.4   Particle size distributions from DLS measurement of a) raw TiO$_2$
powder, TNTs with sonication pretreatment powers of b) 0, c) 7.6, and d)
38.1 W.
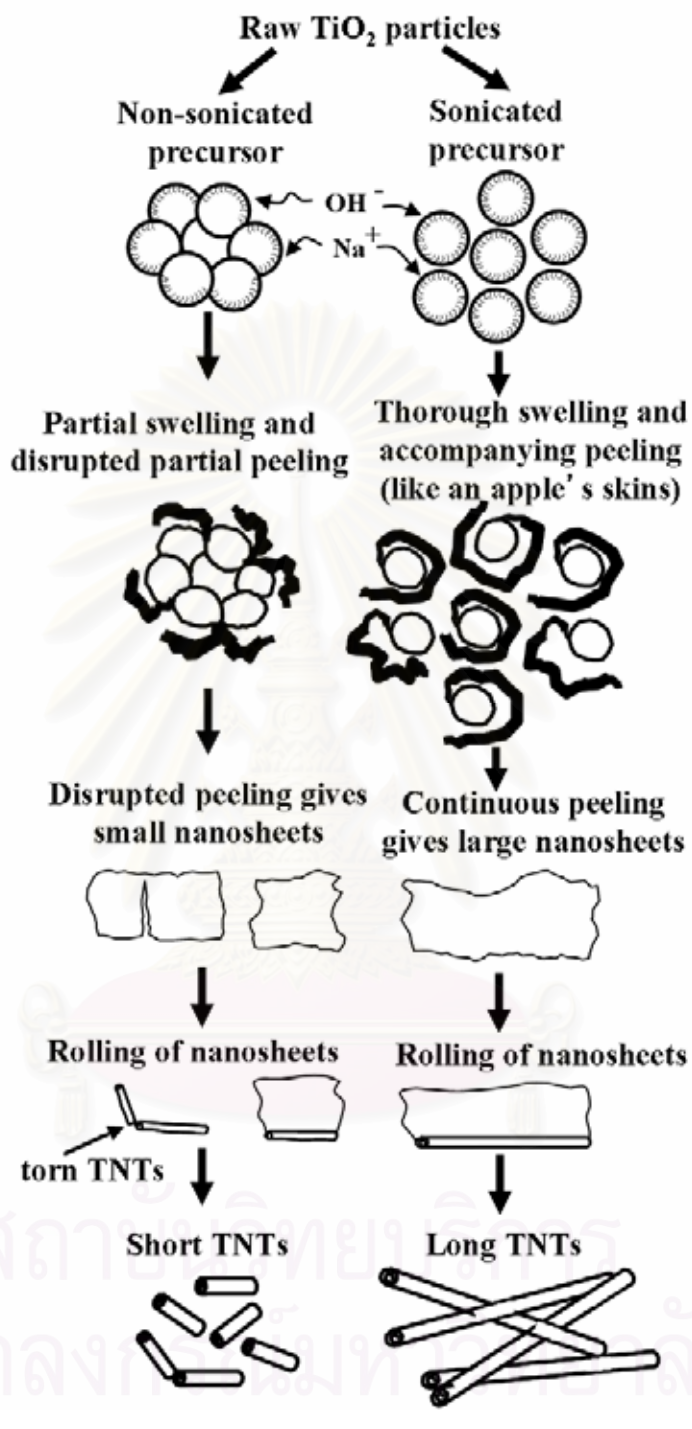
Figure 3.5   Schematic model of the formation of the short TNTs by non-uniform

nanosheet rolling and that of the long TNTs by uniform nanosheet rolling.
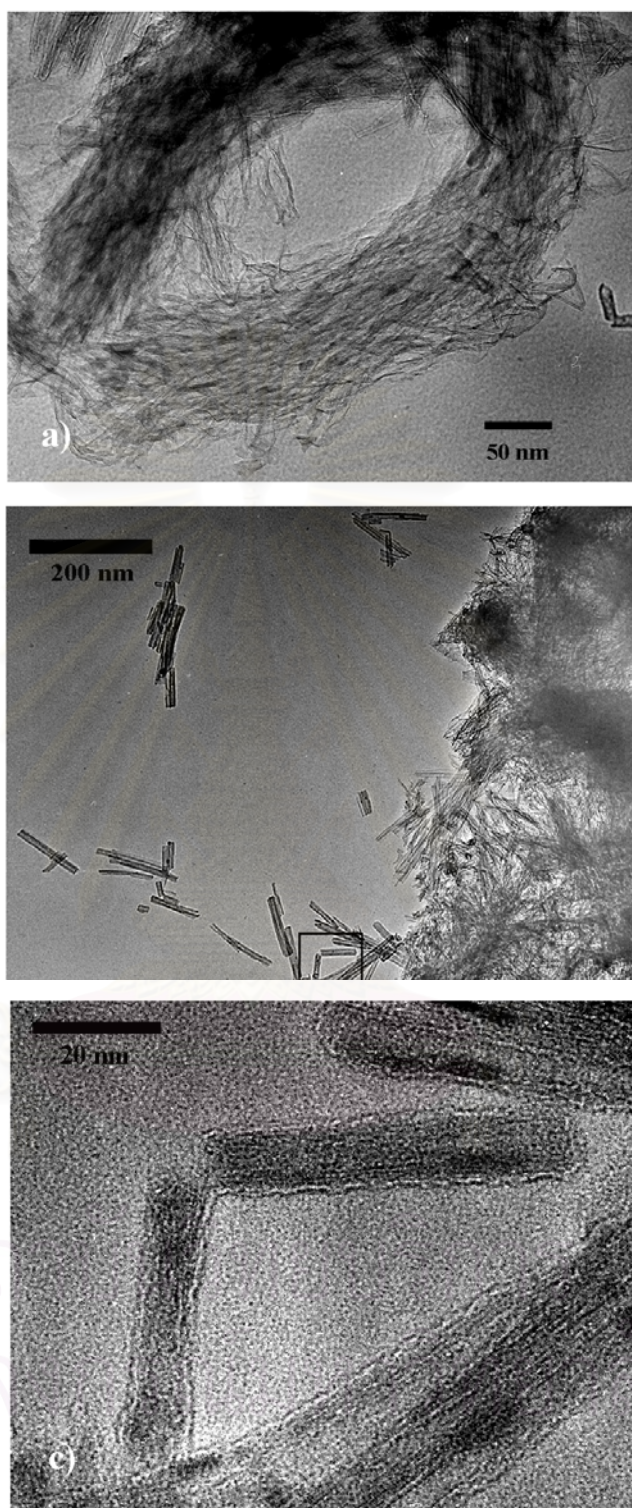
Figure 3.6   TEM images of a) the disordered stacked sheets obtained without sonication pretreatment and left for 1 day and b) short TNTs rolled from the disorder stacked sheets c) partially torn TNTs (shown by a square in figure 3.6b) were obtained with sonication pretreatment and left for 3 days.

CHAPTER IV

INVESTIGATION ON EFFECT OF AVERAGE SIZE OF RAW TITANIA, REACTION TEMPERATURE, SONICATION PRETREATMENT ON TITANATE NANOTUBE AND BROOKITE NANOFIBER IN HYDROTHERMAL REACTION

4.1 Introduction

Recently, hydrothermal method, the soft chemical method, for synthesis of titanate nanostructures, such as titanate nanotubes (TNTs), titanate nanoribbon, titanate nanowire and titanate nanofiber, with high specific surface area has been gaining of great interest from curious researchers (Kasuga et al., 1999; Seo et al., 2001; Yuan and Su, 2004; Viriya-empikul et al., 2008). Several parameters has been investigated, such as reaction temperature, concentration of NaOH, average size of raw TiO_2 powder and sonication pretreatment power (Kasuga et al., 1998; 1999; Ma et al., 2005; Ma et al. 2006; Seo et al., 2001; Weng et al., 2006; Poudel et al., 2005; Yuan and Su, 2004; Viriya-empikul et al., 2008), to find out morphology transformation, specific surface area, phase transition, and so on. However, these reports have been resulted the individual parameter of synthesizing titanate nanostructures. In our previous work, the author subsequently discovered a step towards length control of titanate nanotutes using hydrothermal reaction with sonication pretreatment (Viriya-empikul et al., 2008). When the different reaction temperatures were applied, it has been interesting that the physical properties of titanate nanostructures also differenced between without sonication pretreatment (0 Watt) and applied sonication pretreatment (7.6 Watts).

In this work, the author linked the relationship of three effective parameters, average size of raw TiO_2 powder, reaction temperature, and sonication pretreatment power, and investigated their effects on the specific surface area, morphology and crystalline of titanate product.

4.2 Experimental

Titanate nanostructures were synthesized from 2 types of commercial titania powders, anatase powder (020-78675, KISHIDA, Japan, mean particle size = 400 nm) and rutile powder (224227, Sigma-Aldrich, USA, mean particle size = 1 μm) by hydrothermal process. Raw TiO_2 powder, 0.5 gram, in 50 ml of 10 mol L^{-1} NaOH aqueous solution was sonicated for 8 minutes by a titanium horn in a Teflon vessel. The suspension was placed in a sealed autoclave, and heated in an oven at a constant reaction temperature of interest (90-180 ^oC) for 3 days. After hydrothermal treatment process, the individual samples were filtrated and treated with 0.1 mol L^{-1} HCl solution. Then they were leached with distilled water until the pH of the leaching water reached 7. The leached samples were dried overnight at 70 ^oC in an oven. The authors found that the sonication pretreatment affected to increase length and specific surface area of titanate nanotube synthesized by hydrothermal method at a desired temperature of 150 ^oC (Viriya-empikul et al., 2008). Therefore, the comparison of titanate nanostructure with and without sonication pretreatment at varied reaction temperature was investigated to elucidate their structure and physical properties.

Transmission electron microscope (TEM; JIM2010, JEOL, Japan) was employed to investigate the morphology of synthesized titanate. The difference in crystalline phase of titanate nanomaterials and raw TiO_2 powders was analyzed by X-ray diffractometer (XRD; RINT 2000, Rigaku Co., Japan). The specific surface area of all samples was determined by nitrogen adsorption (BelSorp-Mini II, BEL Japan Inc., Osaka, Japan).

4.3 Results and discussion

4.3.1 Effect of size of raw TiO_2

Titanate nanotubes (TNTs) were fabricated from different average size of raw TiO_2, 400 nm and 1 μm at 150 ^{o}C to investigate their effect. The difference in length and BET surface area of titanate nanotubes synthesized from 400 nm and 1 μm raw powders was shown in Figs. 4.1 and 4.2, respectively. In Fig. 4.1, the similar length (30-200 nm) and diameter (4-6 nm) of titanate nanotube synthesized from 400 nm and 1 μm raw TiO_2 powders were shown. However, the smaller size precursor gave a higher BET surface area titanate than the larger one did as shown in Fig. 4.2. The greater BET surface area indicated the higher yield of titanate nanotubes. On the other hand, the smaller size of TiO_2 particles gave rise to higher reaction rate. It has been reported by Zhu et al. (2005) that the phases of raw TiO2 have no effects on the structures of titanate. Furthermore, Ma et al. (2006) investigated the short time reaction (4 h) of titanate nanotube from different size anatase phase (10 and 200 nm) and found that the titanate nanotube obtained from small raw TiO_2 while the large raw TiO_2 could convert to a sheet like structure with rolled edges and a number of spherical particle remained. Based on TEM observation, the average lengths of TNTs from 400 nm and 1 μm of raw TiO_2 are 79 nm and 143 nm, respectively. It's possible that the TNTs length from large particle is longer than TNTs length from smaller particle. Figure 4.3 shows XRD spectra of raw TiO_2 powder with average size of a) 1 μm and b) 400 nm, titanate nanostructures synthesized from b) at reaction temperature of c) 90, d) 120, e) 150, and g) 180 ^{o}C and titanate nanotubes synthesized from a) at f)150 ^{o}C. In Figs. 4.3 e and f, the characteristic peak around 2θ of 10° of titanate nanotubes synthesized from 400 nm and 1 μm raw TiO_2 powders suggested that the interlayer spacing was not significantly affected by the size of raw material in agreement with previous reports (Suzuki and Yoshikawa, 2004; Viriya-empikul et al., 2008).

4.3.2 Effect of temperature and sonication pretreatment

Regarding the above results, the higher BET surface area titanate nanostructure synthesized from 400 nm raw material should be of interest and selected for further study, due to its greater active sites beneficial for photocatalytic performance. In Figs. 4.4-4.6, it was found that the structure of titanate products and their purity are affected by the reaction temperature and sonication pretreatment. However, the sonication pretreatment affects the product purity fabricated by various reaction temperatures in different ways. At low reaction temperature (90 ^{o}C), only titanate nanotubes, titanate nanosheets, and remaining crystals were observed as shown in Fig. 4.5a. Moreover, the sonication pretreatment was not affected to increase the BET surface area of titanate nanostructures synthesized at 90 ^{o}C as displayed in Fig. 4.6. However, at 120 ^{o}C and 150 ^{o}C mostly titanate nanotube was observed (the remaining crystals was rarely observed) as shown in Fig. 4.4. It was found that the longer length and higher BET surface area of titanate nanotubes were fabricated when sonication pretreatment were applied to the synthesis process. Regarding the formation mechanism of titanate nanotube affected by sonication pretreatment, in the case of without sonication, the Na+ and OH- species could not freely infiltrate into the narrow constricted inter-particle zones and could not thoroughly react with the entire TiO$_2$ surfaces. The small nanosheets were formed and rolled up to form only short TNTs. On the other hand, in the case of the sonicated suspensions, the reaction of NaOH on the surfaces of the deagglomerated TiO$_2$ particles was much more thorough and uniform, and so was the smooth unhindered peeling to form the large nanosheets, which were consequently rolled into long TNTs (Viriya-empikul et al., 2008). When the reaction temperature increased up to 180 ^{o}C, only titanate nanofiber was formed as displayed in Figs. 4.5b and 4.5c and, in Fig. 4.6, the BET surface area of titanate nanofiber was not significantly different. Note that titanate nanotube synthesized at 150 ^{o}C with sonication pretreatment showed the highest BET surface area.

XRD was also used to confirm the structure of titanate nanomaterials. The XRD patterns of the nanomaterials at different reaction temperatures are shown in Fig. 4.3. The prominent peak at 10°, indicating the appearance of layered portonic behavior (Feist and Davies, 1992; Suzuki and Yoshikawa, 2004), was observed. It was found that titanate nanostructure with anatase phase could be obtained only at the reaction

temperature of 90 ^{o}C. The peak around 2θ of 10° of the titanate nanomaterials slightly shifted to the right when the reaction temperature increased up to 150 ^{o}C.

4.3.3 Anatase-brookite phase transformation in synthesis of titanate nanofiber

Figure 4.7 depicts XRD patterns of titanate nanofibers synthesis with and without sonication pretreatment at 180 ^{o}C. The XRD pattern of titanate nanofibers synthesized with and without sonication shows the differences in XRD pattern, indicating that the new phase was formed and/or the sample has become more crystallized, though all samples were not shown the significantly different properties as observed by TEM (Figs. 4.5b and 4.5c) and nitrogen adsorption (Fig. 4.6). Increase in an input power of sonication gives rise to higher intensity of the new peaks. The shifting peak around 2θ of 10° was observed, though this phenomena was not found in other morphology. By comparing XRD patterns of titanate nanofibers with database of XRD pattern of rutile phase, anatase phase and brookite phase from JCPDS 34-0180, 02-0406, and 29-1360, respectively, XRD pattern of titanate nanofiber synthesized with sonication pretreatment matched well with the XRD database of brookite phase. Meng et al. (2004) has been reported the XRD pattern of raw brookite TiO$_2$ and titanate nanowires. The XRD peak pattern of titanate nanowire has been shown the similar peak of our titanate nanofiber synthesized with sonication pretreatment (in Fig. 4.7). However, the titanate nanofiber synthesized at 180 ^{o}C still remained titanate peak (around 2θ = 10°).
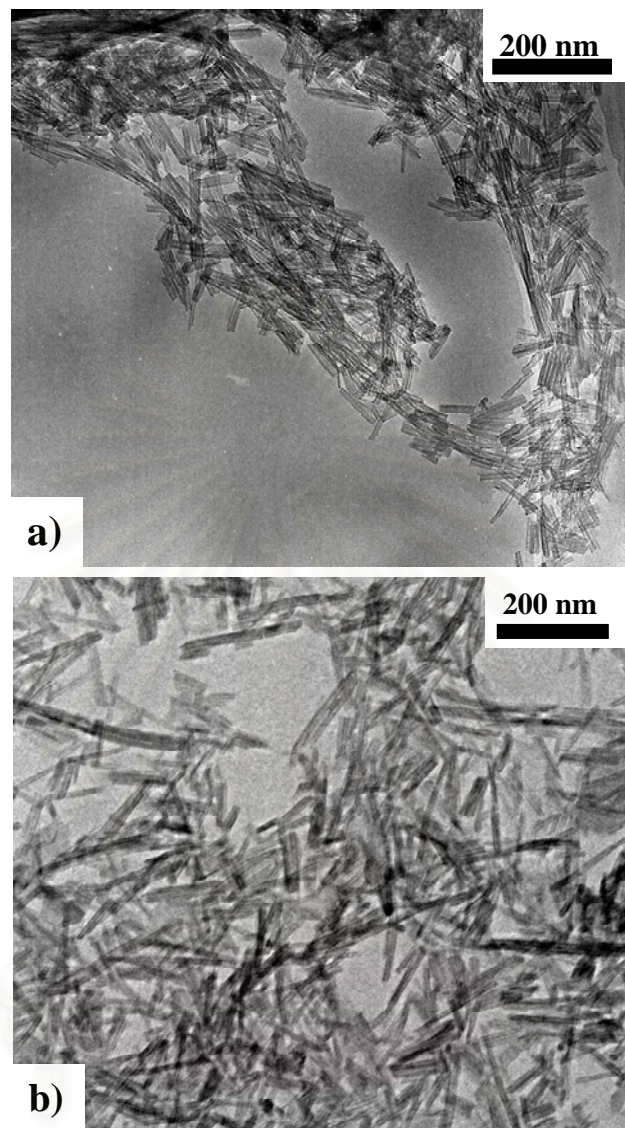
Figure 4.1 TEM images of titanate nanotubes synthesized from TiO$_2$ having average size 400 nm and 1 μm at reaction temperature of 150 ^{o}C without sonication pretreatment
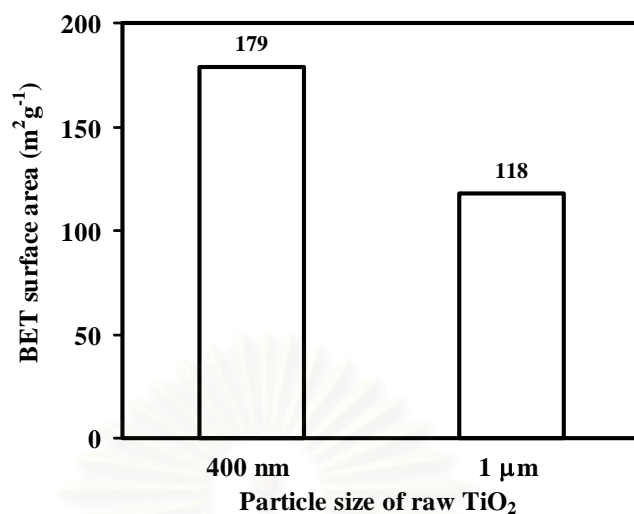
Figure 4.2 BET surface area of titanate nanotubes synthesized from raw TiO_2 having average size 400 (8.3997 m^2g^{-1}) nm and 1 μm (1.7278 m^2g^{-1}) at reaction temperature of 150 ^oC without sonication pretreatment
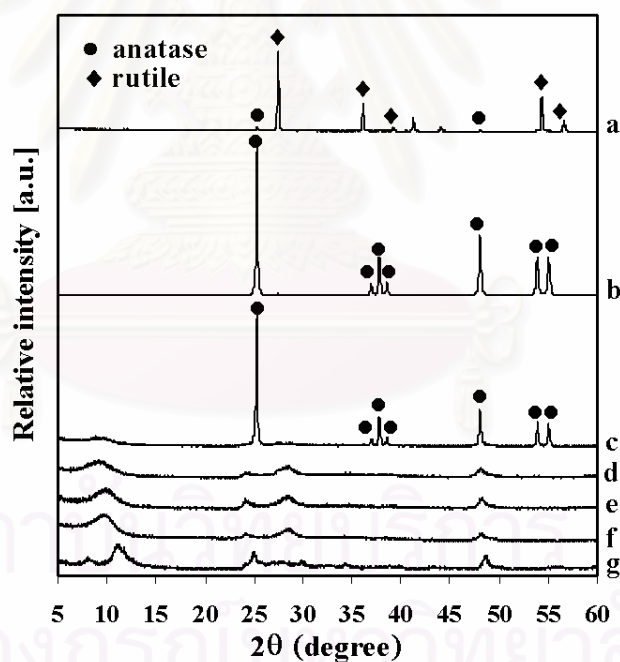
Figure 4.3 XRD spectra of raw TiO_2 powder with average size a) 1μm and b) 400nm, titanate nanostructures synthesized (from 400nm raw TiO_2) at reaction temperature of c) 90, d) 120, e) 150 and g) 180 ^oC and titanate nanotubes synthesized (from 1μm raw TiO_2) at f)150^oC.
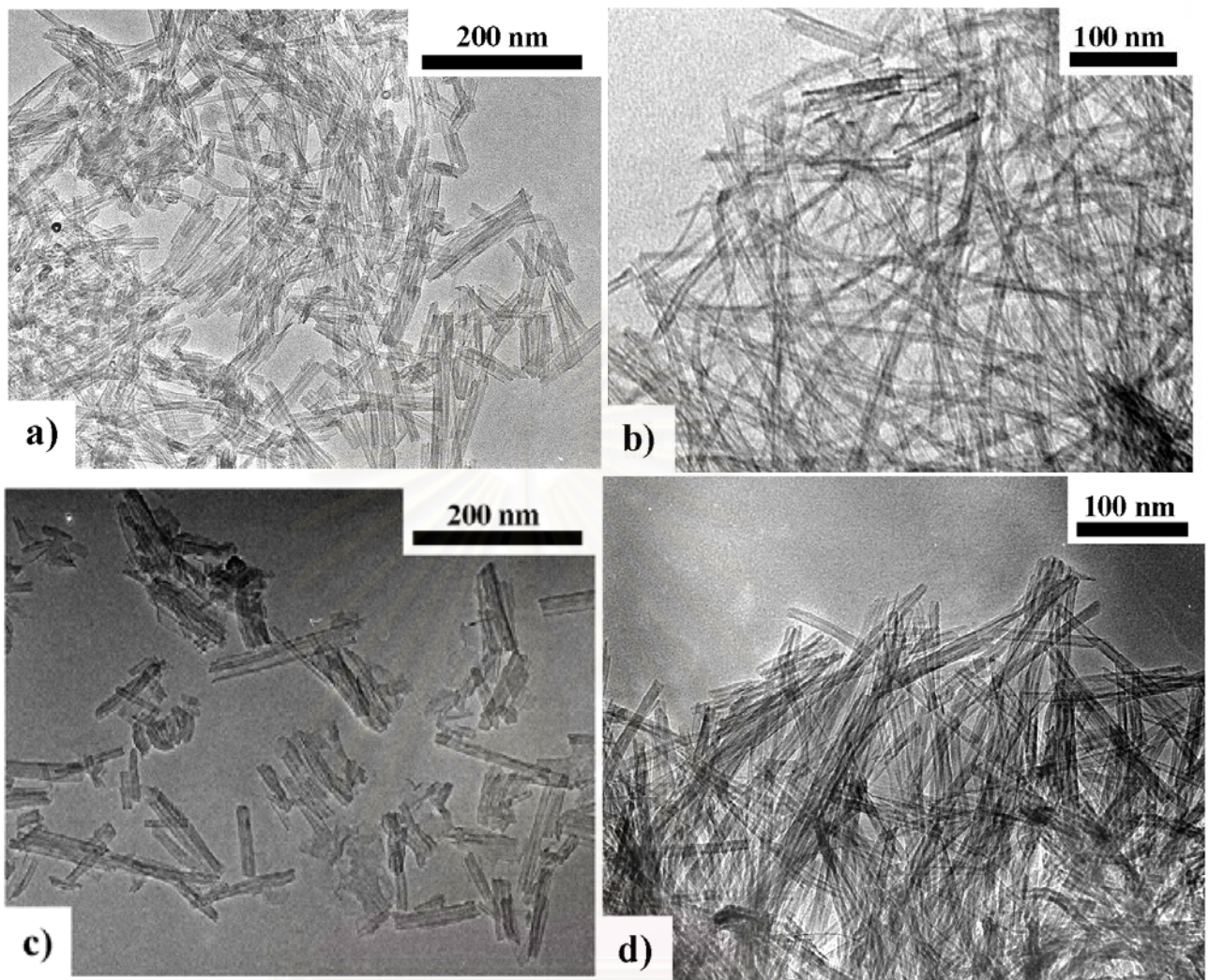
Figure 4.4 TEM images of titanate nanotubes (from 400nm raw TiO_2) prepared at
reaction temperature of $120^{\circ}C$ with sonication power of a) 0, b) 7.6 Watts
and at reaction temperature of $150^{\circ}C$ with sonication power of c) 0, d) 7.6
Watts.
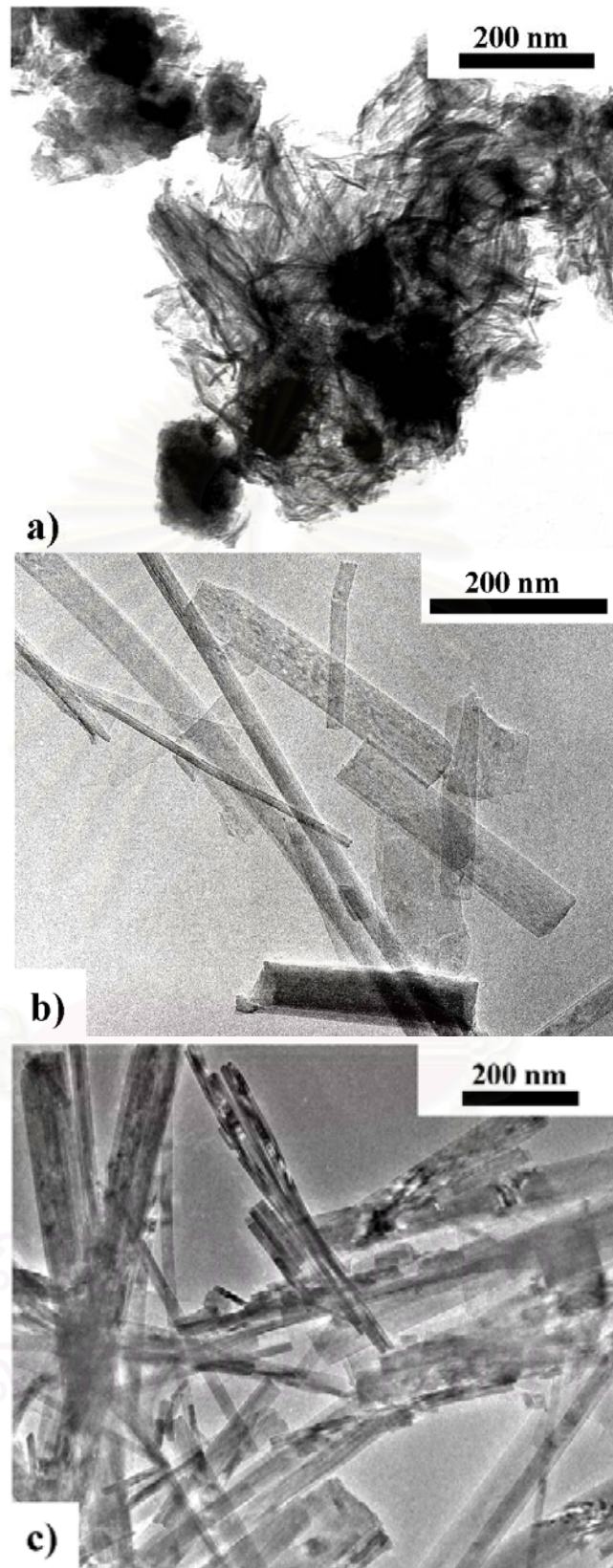
Figure 4.5 TEM images of titanate nanostructures synthesized (from 400nm raw TiO$_2$) at reaction temperature of a) 90°C and titanate nanofibers synthesized at 180 ^{o}C with sonication power of b) 0 and c) 7.6 W.
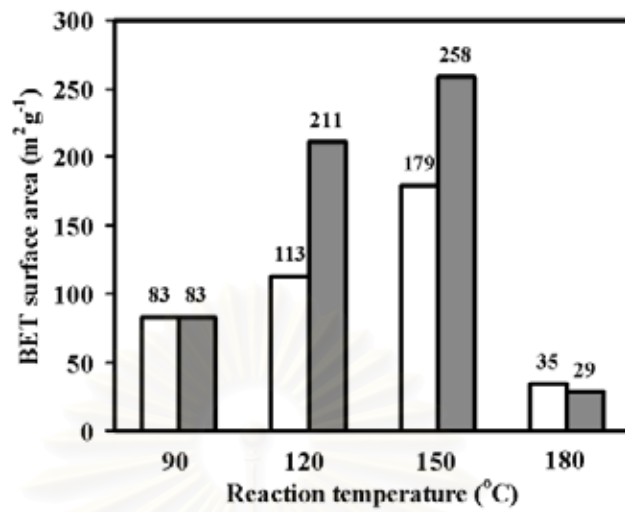
Figure 4.6 BET surface area of titanate nanostructures synthesized (from 400nm
raw TiO_2) at reaction temperature of a) 90, b) 120, c) 150 and d) 180°C
with sonication power of (□) 0 and (■) 7.6 Watts
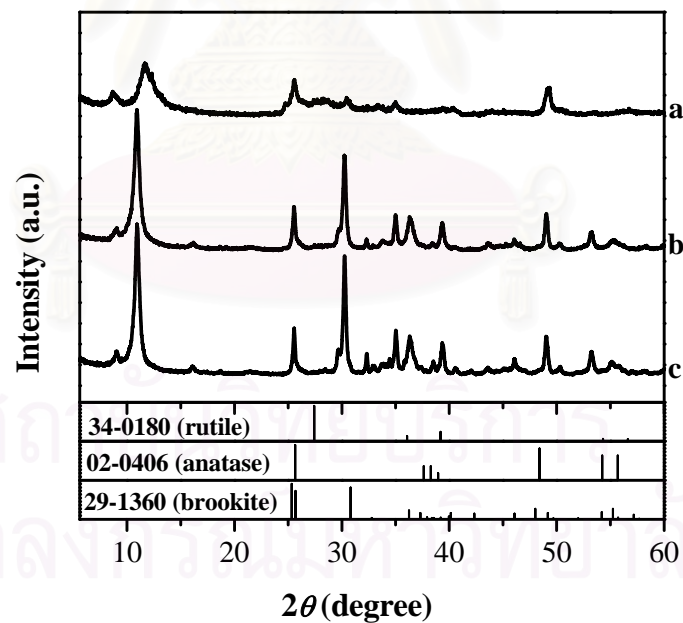
Figure 4.7 XRD spectra of titanate nanofiber synthesized (from 400nm raw TiO_2) at
reaction temperature of 180 ^{o}C with sonication power of a) 0, b) 7.6 and c)
38.1 Watts.

CHAPTER V

EXAMINATION OF PHOTOCATALYTIC AND UV ADSORPTION PROPERTIES OF TITANATE NANOSTRUCTURES SYNTHESIZED BY HYDROTHERMAL PROCESS

5.1 Introduction

Titanium dioxide (TiO_2) is widely used as photocatalyst (Nader, 2004; Kaneco et al., 2004; Chen et al., 2002; Zhao et al., 2004; Leng et al., 2003; Kanki et al., 2005; Nonami et al., 2004; Ao and Lee, 2005) due to its relatively low price, non-toxicity, high chemical stability, etc. In nature, TiO_2 has three crystallite phases, namely, anatase, rutile, and brookite. However, the anatase phase of TiO_2 exhibits a higher photocatalytic activity than that of the other two. The anatase TiO_2 has an energy band gap of 3.2 eV, thereby allowing it to absorb light with wavelength shorter than ca. 390 nm (Nader, 2004; Kaneco et al., 2004; Chen et al., 2002; Zhao et al., 2004; Leng et al., 2003). In order to increase its performance, many attempts are made to increase the specific surface area of TiO_2 nanostructures (Imai et al., 1999; Gopal et al., 2005; Dmitry et al., 2006; Kasuga et al., 1998; 1999; Viriya-empikul et al., 2008) by template replication and hydrothermal techniques. With the template replication method, well aligned and uniform TiO_2 nanotubes were reported (Imai et al., 1999; Gopal et al., 2005). However, there is difficulty in separating the tubular product from the residual template materials (Dmitry et al., 2006). In comparison, the hydrothermal technique (Kasuga et al., 1998; 1999; Viriya-empikul et al., 2008) which converts TiO_2 powders to titanate nanostructures in an alkali solution could reportedly provide slender titanate nanostructures. In our previous work, the sonication pretreatment was applied to increase the length and specific surface area of titanate nanotube via hydrothermal synthesis (Viriya-empikul et al., 2008).

The degradation of organic pollutants in gas or liquid phases is generally employed to determine the photocatalytic activity of TiO_2 nanostructures (Nader, 2004; Kaneco et al., 2004; Chen et al., 2002; Zhao et al., 2004; Leng et al., 2003;

Kanki et al., 2005; Nonami et al., 2004; Ao and Lee, 2005). Photocatalytic degradation of various organic compounds under influences of key parameters such as reaction temperature (Kaneco et al., 2004), pH (Kaneco et al., 2004; Chen et al., 2002; Zhao et al., 2004; Swarnalatha and Anjaneyulu, 2004), irradiation period (Swarnalatha and Anjaneyulu, 2004), initial concentration of pollutant (Kaneco et al., 2004; Ao and Lee, 2005; Swarnalatha and Anjaneyulu, 2004; Hegedus and Dombi, 2004), light intensity (Kaneco et al., 2004; Zhang et al., 2001; Chun et al., 2000) and catalyst concentration (Kaneco et al., 2004; Swarnalatha and Anjaneyulu, 2004; Irmak et al., 2004; Qamar et al., 2005) have been reported. However, there is only limited examination of relevance among the titanate nanostructure characteristics and their photocatalytic activities and UV absorption in comparison with anatase and rutile titania. In this work, particle morphology, specific surface area, XRD pattern and energy band gap of the titanate nanostructures synthesized by hydrothermal process were investigated and related to their photocatalytic activity in comparison with those of TiO_2 anatase and rutile phases.

5.2 Experimental

5.2.1 Synthesis and characterization of titanate nanostructure

Titanate nanostructures were synthesized from commercial titania powders (020-78675, KISHIDA, Japan, anatase phase) by hydrothermal process. TiO_2 powder, 0.5 gram, in 50 ml of 10 mol/L NaOH aqueous solution was sonicated for 8 minutes by a titanium horn in a Teflon vessel. The suspension was placed in a sealed autoclave and heated in an oven at a constant reaction temperature of interest (90-150 ^{o}C) for 3 days. After hydrothermal treatment process, the individual samples were filtrated and treated with 0.1 mol/L HCl solution. Then they were leached with distilled water until the pH of the leaching water reached 7. The leached samples were dried overnight at 70 ^{o}C in an oven. It has been reported that sonication power could exert significant influence on titanate nanostructure and increase in specific surface area (Viriya-empikul et al., 2008). Therefore, the fabrication of titanate nanostructures with sonication pretreatment at each reaction temperature was investigated to elucidate their structure and physical properties.

The microstructure of synthesized titanate was analyzed by Transmission electron microscope (TEM; JIM2010, JEOL, Japan). The X-ray diffractometer (XRD; RINT 2000, Rigaku Co., Japan) was used to investigate the difference of crystalline phase of titanate nanomaterials and TiO_2 raw powders. The specific surface area of all samples was determined by nitrogen adsorption (BelSorp-Mini II, BEL Japan Inc., Osaka, Japan). The ultraviolet–visible reflectance of the samples was obtained by a UV–vis spectrometer (Lambda 650, Parkin Elmer Inc., USA).

5.2.2 Photocatalytic experiments and analysis

Raw TiO_2 powder and titanate nanostructures produced at different temperatures (90-150°C) were employed to decompose phenol, which is considered as a model organic compound, within a shaking slurry photoreactor under UV irradiation. 2 mg of the particulate suspended in 20 ml of 10 ppm phenol solution in quartz test tubes were used in each experiment. The suspension was irradiated with two 30-Watt UV-C lamps (Philips G30T8) with a radiation peak at 253.7 nm (4.89 eV) and mechanically shaken to ensure uniform dispersion of the synthesized powder in each test tube at a room temperature. To distinguish the intrinsic effect of phenol adsorption on the powder surface, blank experiments were conducted without UV-C irradiation.

The suspension was filtered with 0.45 µm millipore filter membrane before analyzing. The residual concentration of phenol in the supernatant liquid was then analyzed by high-performance liquid chromatography (HPLC, Shimadzu LC-10ADVP FCV-10ALVP 2005, Kyoto, Japan) using a Phenomenex column (C18, length = 150 mm; internal diameter = 4.6 mm; particle diameter = 5 µm), with 25% acetronitrile and 75% water as the mobile phase. The UV-vis detector with UV spectrum of 254 nm was employed. The column temperature was 30 ^{o}C. The flow rate of the mobile phase was 0.6 cm^3min^{-1} with an injection volume of 10 µL. The total organic carbon (TOC) in the phenol solution was also measured using total organic carbon analyzer (Shimadzu TOC VCPH, Kyoto, Japan).

5.3 Results and discussion

5.3.1 Titanate nanostructures

Typical titanate nanostructures fabricated by hydrothermal process at the reaction temperature of 90 ^{o}C to 150 ^{o}C were depicted in Figure 5.1. The TEM micrograph (Fig. 5.1a) reveals a mixture of titanate nanotubes, titanate nanosheets and remaining crystals fabricated at 90 ^{o}C. At the reaction temperature of 120 and 150 ^{o}C, only titanate nanotube structures were produced as shown in Figures 5.1b and 5.1c. The effect of reaction temperature on the morphology of titanate nanostructures has been reported (Yuan and Su, 2004; Ma et al., 2005). Typically, hydrothermal reaction between TiO_2 particles and NaOH solution could be initialed when the reactive Na+ and OH- species diffuse to the surface of the TiO_2 particles, resulting in the formation of titanate nanosheet peeling from the reactant TiO_2 particle surface. TEM images of TiO_2 nanoparticle swelling and titanate nanosheets peeling off from swollen TiO_2 particle were provided as evidences by Yang et al. (2003). Based on Arrhenius hypothesis, the formation rate of titanate nanosheet would be higher when the reaction temperature increased, leading to a higher peeling rate of titanate nanosheet, thereby increasing the formation rate of titanate nanotube.

The specific surface area of titanate nanostructures was significantly larger compared with that of titania raw powder as summarized in Table 1. Titania raw powder has the BET surface area of ca. 8 m^2g^{-1}. After hydrothermal reaction, BET surface area of titanate nanostructures synthesized at 90, 120 and 150 ^{o}C were drastically increased to 83, 211 and 258 m^2g^{-1}, respectively.

It is often assumed that increasing the BET surface area of the titanate nanostuructures would automatically provide many more active sites beneficial for photocatalytic performance. However, in Figure 5.2, the XRD peek of anatase phase in the titanate nanostructures synthesized at 90 ^{o}C a remarkably decreased. Additionally, the anatase peak (2θ = 24.5 ^{o}) disappeared from the titanate nanostructures synthesized at the reaction temperature of 120 ^{o}C and 150 ^{o}C. This reduction in the anatase phase would lead to the decrease in the photocatalytic performance of the synthesized titanate nanostructures. In Figure 5.2, the authors also

observed the representative peak of titanate nanostructures appeared at around $2\theta = 10^o$ under every condition of hydrothermal process as reported by Suzuki and Yoshikawa (2004).

In Figure 5.3, the reflectance of compressed sheets made of anatase TiO_2 (raw powder), rutile TiO_2 (224227, SIGMA-ALDRICH, USA.) and titanate nanosturctures was analyzed by UV/vis spectrometer. The band gap energy listed in Table 5.2 was calculated according to the described procedure (Sanchez and Lopez, 1995). The band gap energies of titania anatase phase (3.2 eV) and rutile phase (3.0 eV) were essentially the same as reported (Diebold, 2003). After hydrothermal process, the band gap energy of titanate nanostructures was increased from the raw material. When the hydrothermal reaction temperature was increased, the band gap energy of titanate nanostructures followed suit. However, at the reaction temperatures of 120 ^{o}C and 150 ^{o}C, the two listed values were more or less equal. This slightly different band gap energy was consistent with the fact that the shape of samples (nanotube) and physical properties (BET surface area and XRD peak) in Table 5.1 and Figures 5.1b, 5.1c and 5.2 are similar. Meanwhile, titanate nanostructure synthesized at reaction temperature of 90 ^{o}C was clearly different from the other cases, especially the difference in the XRD peaks. Since the titanate sample synthesized at 90 ^{o}C was a mixture of titanate nanosheet, titanate nanotube and remaining crystals, the reflectance curve or band gap energy of the sample should lie between the titanate and crystals (Ma et al., 2005).

5.3.2 Photocatalytic activity

The decomposition of phenol by 253.7 nm-UV (Kanki et al., 2005; Chun et al., 2000) was employed to investigate and compare the photocatalytic performance of the raw titania powder and titanate nanostructures. The curves of normalized residual phenol and TOC concentrations decomposed with UV light only, raw titania powder and titanate nanostructures (produced at reaction temperature of 90 ^{o}C, 120 ^{o}C, and 150 ^{o}C) enhanced with UV light at various irradiation times were shown in Figure 5.4. The decreases in normalized concentrations in the case of raw titania powder enhanced with UV light were fastest. Interestingly, the case of titanate nanostructures enhanced with UV light showed the poorest photocatalytic activity, even lower than

the case of UV light only. Since the BET surface area of titanate nanostructures was higher than that of the raw titania powder by 4 to 30 times, whereas the crystalline peak of TiO_2 anatase phase became lower at synthesized reaction temperature of 90 ^{o}C and totally disappeared at the higher synthesized reaction temperatures, this means that the photocatalytic activity was more dominated by the anatase phase than the BET surface area (Imai et al., 1999). From Table 5.2, although the UV light source to activate the photocatalytic reaction was higher than the band gap energy, the photocatalytic activity of titanate nanostructure was not observed. As mentioned above, based on the XRD analyses, the titanate nanostructures show lower semiconductivity behavior, regarding to the disappearance of the XRD peak at 2θ = 24.5 ^{o} (Swarnalatha and Anjaneyulu, 2004). In Figure 5.3, the anatase TiO_2 adsorbed a higher energy of UV light than the rutile TiO_2. In addition, the former can generate strong radicals to decompose phenol around the anatase TiO_2 particles as shown in Figure 5.4. The UV/vis and phenol degradation results show that the titanate nanostructure was more effective in UV light adsorption but less decomposition effect than the rutile and anatase phases. As the prime summary of this investigation, the above results indicated that the titanate nanostructures are better than TiO_2 as UV protector.

Table 5.1 BET surface area of titanate nanostructures as a function of reaction temperature

Reaction temperature (^{o}C)	90	120	150
BET surface area (m^2g^{-1})[a]	83	211	258
Shape	nanosheet, nanotube, remaining crystal	nanotube	nanotube

[a]TiO_2 raw powder = 8 m^2/g

Table 5.2 Band gap values for the titania and titanate nanostructures

Sample	Band gap (eV)
TiO_2 anatase phase powder	3.33
Synthesized titanate at 90°C	3.44
Synthesized titanate at 120°C	3.84
Synthesized titanate at 150°C	3.81
TiO_2 rutile phase powder	3.06
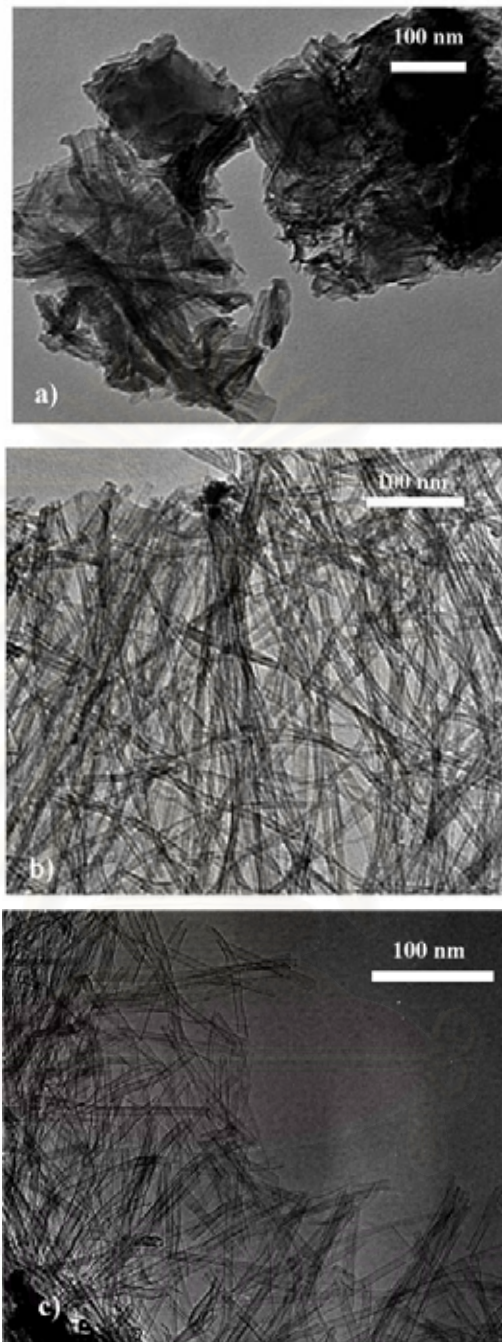
Figure 5.1 TEM image of titanate nanostructures produced at reaction temperature of
a) 90°C, b) 120°C and c) 150°C
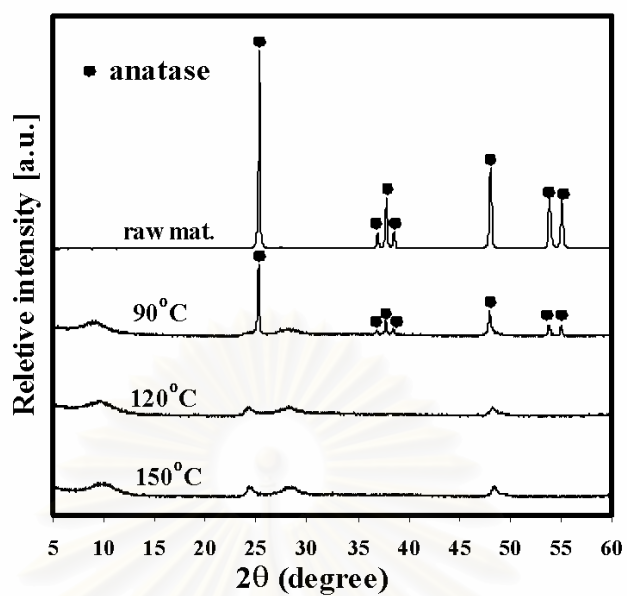
Figure 5.2   XRD spectra of raw TiO$_2$ powder, titanate nanostructure produced at
reaction temperature of 90°C, 120°C, and 150°C
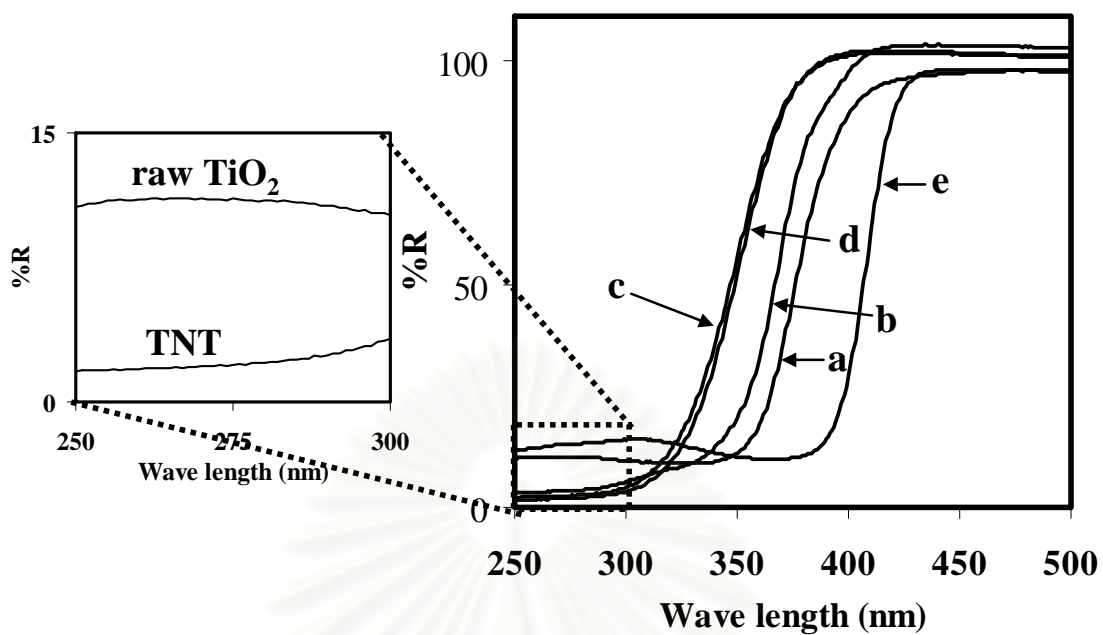
Figure 5.3 UV–vis reflectance spectrum patterns of a) raw TiO$_2$ anatast phase
powder, titanate nanostructure produced at reaction temperature of b)
90°C, c) 120°C, and d) 150°C and e) TiO$_2$ rutile phase powder

a)

b)
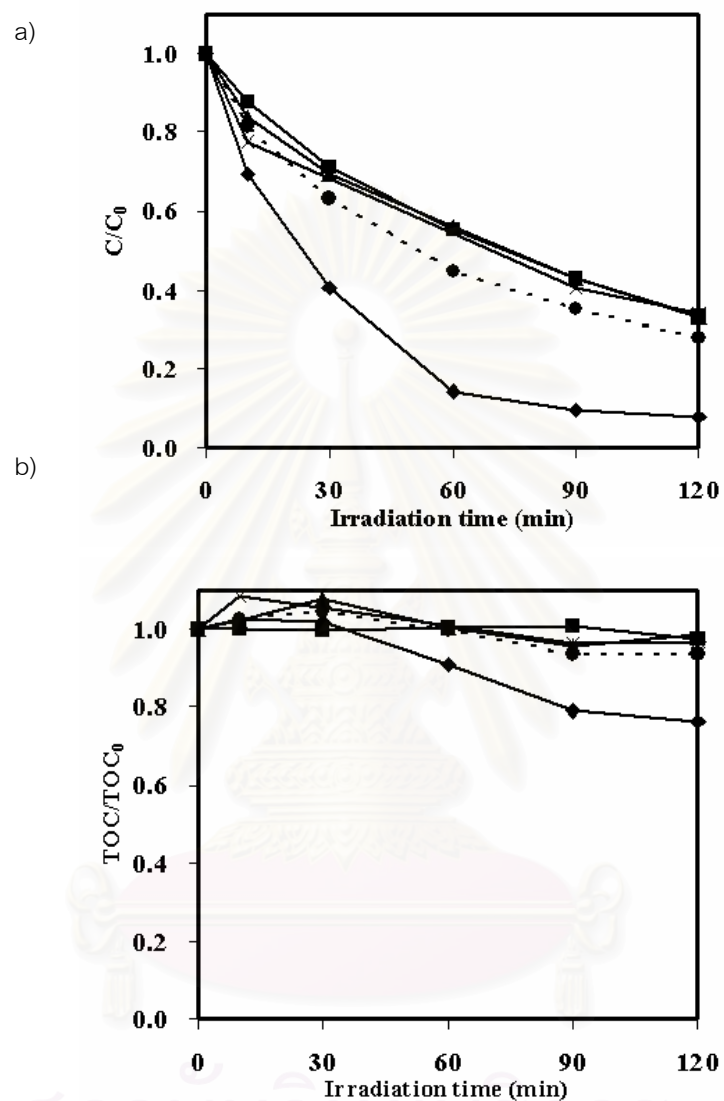
Figure 5.4 Change of normalized concentration of a) phenol and b) TOC decomposed
by employing UV irradiation only (●), UV+TiO$_2$ raw powder (◆),
UV+titanate nanostructures produced at reaction temperature of 90°C (■),
120°C (▲), and 150°C (✕)

CHAPTER VI

CONCLUSIONS AND RECOMMENDATIONS

6.1 Conclusions

This work is focusing on investigation of new nanostructure of titanium compound and its properties. A step-by-step investigation of synthesis and application has been conducted and then divided into 3 parts, which could be summarized as follows,

6.1.1 Investigation for length control of titanate nanotubes using hydrothermal reaction with sonication pretreatment

A significant step towards the length control of TNTs synthesized by a typical hydrothermal process has been achieved by applying low-power sonication pretreatment. Generally, the average length of TNTs without sonication pretreatment was approximately 53 nm. In contrast, a larger number of significantly longer TNTs with average hydrodynamic diameters of 490 and 1760 nm were produced when the sonication power was 7.6 and 38.1 Watts, respectively. Based on the published mechanisms (Yuan and Su, 2004; Yang et al., 2003; Du et al., 2001; Wang et al., 2002; Zhang et al., 2003; Thorne et al., 2005; Dmitry et al., 2004) and our TEM images taken at different reaction times, the authors could successfully explain how the sonication pretreatment contributed to the length control of the TNTs.

6.1.2 Investigation on effect of average size of raw titania, reaction temperature, sonication pretreatment on titanate nanotube and brookite nanofiber in hydrothermal reaction

The three parameters were employed to observe the morphology, BET surface area, and crystalline phase of titanate nanostructures. The largest BET surface area

$(258 \text{ m}^2\text{g}^{-1})$ of titanate product was obtained by smaller TiO_2 raw powders (400 nm) at 150 $^{\circ}$C reaction temperature with sonication pretreatment. The low BET surface area of titanate nanostructure occurred when the reaction temperature reached to 180 $^{\circ}$C or the morphology of titanate product was nanofiber. Based on XRD measurement, the crystalline phase (anatase or rutile phase) was disappeared after hydrothermal reaction. However, titanate nanofiber obtained after applying sonication pretreatment showed the XRD peak pattern different from other morphology and also showed brookite phase.

6.1.3 Examination of photocatalytic and UV adsorption properties of titanate nanostructure synthesized by hydrothermal process

Titanate nanostructure with tubular morphology could be successfully synthesized by the hydrothermal reaction of raw TiO_2 powder. By increasing the hydrothermal reaction temperature, the BET surface area of the titanate nanostructure was drastically increased by 4 to 30 times of the raw titania powder. It was found that the anatase peak was hardly observable in every sample of the synthesized titanate nanostructure. Though the investigation of photocatalytic activity based on phenol decomposition revealed that the titanate nanostructure which was activated by UV-C light could provide no intrinsic photocatalytic activity toward phenol, the synthesized titanate exhibited high UV adsorption capability.

Finally, the authors could summarize that the results of this research could fulfill the proposed objectives which include the fact that the titanate nanoroll could be synthesized by micron-sized TiO_2 powder and the morphology, size, and specific surface area of titanate product could be investigated in interesting conditions.

6.2   Recommendations for Future Work

The authors found that the parameter to control length of titanate nanotube is sonication power. Because of the unknown parameters at the peeling step, the theory of wide : length ratio and rolling direction of titanate nanosheet is not clear. The research should be expanded to the simulation W:L ratio and rolling direction of titanate nanosheet to form titanate nanotube.

By the photocatalytic activity of titanate nanostructures, there are two possible ways to pursue this research work further. On one hand, since the titanate material shows the UV protection property (protect the phenol decomposition from UV), it's possible to apply this material with the sun screen application. On the other hand, because the titanate nanotube shows the high specific surface area, the improving of phase structure (anatase) would be expected to increase photocatalytic activity.

Furthermore, thermal post-treatment and hydrothermal post-treatment are two methods to transform the titanate material to TiO_2 (anatase phase). However, the authors are interested in hydrothermal post-treatment because the thermal post-treatment breaks the morphology of titanate nanotube to spherical shape (very low surface area) and sodium ion is still remained in side the TiO_2. On the other hand, the hydrothermal post-treatment changes the morphology of titanate nanotube to leaf shape or rice shape of TiO_2 (anatase phase and quite high surface area) and sodium ion inside titanate nanostructure is also removed. This idea (hydrothermal post-treatment) has been by Yan et al. (2007) already. However, Yan et al. reported that the product was anatase/ titanate nanotube composite but the authors think that if all titanate nanotube is transform to rice shape of TiO_2, the photocatalytic activity will be much increase.

REFERENCES

Ao, C.H.; Lee, S.C. Indoor air purification by photocatalyst TiO_2 immobilized on an activated carbon filter installed in an air cleaner. Chem. Eng. Sci. 60 (2005): 103-109.

Bavykin, D.V.; Friedrich, J.M.; Walsh, F.C. Protonated Titanates and TiO_2 Nanostructured Materials: Synthesis, Properties, and Applications. Adv. Mater. 18 (2006): 2807.

Bavykin, D.V.; Parmon, V.N.; Lapkin, A.A.; Walsh, F.C. The effect of hydrothermal conditions on the mesoporous structure of TiO_2 nanotubes. J. Mater. Chem. 14 (2004): 3370.

Boer, K W. Survey of Semiconductor Physics. Van Nostrand Reinhold: New York, 1990.

Borgarello, E., Kiwi, J., Pelizzetti, E., Visca, M., and Gratzel, M. Photochemical cleavage of water by photocatalysis. Nature. 289 (1981): 158.

Cai, R. X., Kubota, Y., Shuin, T., Sakai, H., Hashimoto, K, Fujishima, A. Induction of cytotoxicity by photoexcited TiO_2 particles. Cancer Res. 52 (1992): 2346-2348.

Chakrabarti, S.; Dutta, K.B. Photocatalytic degradation of model textile dyes in wastewater using ZnO as semiconductor catalyst. J. Hazard. Mater. B 112 (2004): 269-278.

Chen, J.; Eberlein, L.; Langford, C.H. Pathways of phenol and benzene photooxidation using TiO_2 supported on a zeolite. J. Photochem. Photobiol. A: Chem. 148 (2002): 183-189.

Cheng, H., Ma, J., Zhao, Z., and Qi, L. Hydrothermal Preparation of Uniform Nanosize Rutile and Anatase Particle. Chem. Master. 7 (1995): 663-671.

Chun, H.; Yizhong, W.; Hongxiao, T. Destruction of phenol aqueous solution by photocatalysis or direct photolysis. Chemosphere 41 (2000): 1205-1209.

Daneshvar, N.; Salari, D.; Khataee, A.R. Photocatalytic degradation of azo dye acid red 14 in water on ZnO as an alternative catalyst to TiO_2. J. Photoch. Photobio. A 162 (2004): 317-322.

Diebold, U. The surface science of titanium dioxide. Surf. Sci. Rep. 48 (2003): 53-229.

Dmitry, V. B.; Jens, M.F.; Frank, C.W. Protonated Titanates and TiO_2 Nanostructured Materials: Synthesis, Properties, and Applications. <u>Adv. Mater.</u>, 18 (2006): 2807-2824.

Du, G.H.; Chen, Q.; Che, R.C.; Yuan, Z.Y.; Peng, L.M. Preparation and structure analysis of titanium oxide nanotubes <u>Appl. Phys. Lett.</u> 79 (2001): 3702-3704.

Duonghong, D., Borgarello, E., and Gratzel, M. Dynamics of light-induced water cleavage in colloidal systems. <u>J. Am. Chem. Soc.</u> 103 (1981): 4685.

Feist P.T.; Davies K.P. The Soft Chemical Synthesis of TiO_2 (B) from Layered Titanates. J. Solid State Chem. 101 (1992): 275-295.

Fox, M.A. and Dulay, M.T. Heterogeneous Photocatalysis. <u>Chem. Rev.</u> 93 (1993): 341-357.

Fujishima, A.; Rao N.T.; Tryk, A. D. Titanium dioxide photocatalysis. <u>J. Photochem. Photobio. C</u> 1 (2000): 1-21.

Gerischer, H. and Heller, A. Photocatalytic oxidation of organic molecules at TiO_2 particles by sunlight in aerated sea water. <u>J. Electrochem. SOC.</u> 139 (1992): 113-118.

Gopal, K.M.; Karthik, S.; Maggie, P.; Oomman, K.V.; Craig, A.G. Enhanced Photocleavage of Water Using Titania Nanotube Arrays Nano Lett. 5 (2005): 191-195.

Gratzel, M. Artificial photosynthesis: water cleavage into hydrogen. and oxygen by visible light. <u>ACC. Chem. Res.</u> 14 (1981): 376.

Hegedus, M.; Dombi, A. Gas-phase heterogeneous photocatalytic oxidation of chlorinated ethenes over titanium dioxide: perchloroethene. <u>Appl. Catal. B: Environ.</u> 53 (2004): 141-151.

Idakieva, V.; Yuan, Z.Y.; Tabakova, T.; Su, B.L. Titanium oxide nanotubes as supports of nano-sized gold catalysts for low temperature water-gas shift reaction. <u>Appl. Catal. A: General</u> 281 (2005): 149–155.

Imai, H.; Takei, Y.; Shimizu, K.; Matsuda, M.; Hirashima, H. Direct preparation of anatase TiO_2 nanotubes in porous alumina membranes. <u>J. Mater. Chem.</u> 9 (1999): 2971-2972.

Ireland, J. C., Klostermann, P., Rice, E. W., Clark, R. M. Inactivation of Escherichia coli by titanium dioxide photocatalytic oxidation. Appl. Environ. Microbiol. 59 (1993): 1668-1670.

Irmak, S.; Kusvuran, E.; Erbatur, O. Degradation of 4-chloro-2-methylphenol in aqueous solution by UV irradiation in the presence of titanium dioxide. Appl. Catal. B: Environ. 54 (2004): 85-91.

Jackson, N. B., Wang, C. M., Luo, Z., Schwitzgebel, J., Ekerdt, J. G., Brock, J. R., and Heller, A. Attachment of TiO_2 powders to hollow glass microbeads: activity of the TiO_2-coated beads in the photoassisted oxidation of ethanol to acetaldehyde. J. Electrochem. SOC. 138 (1991): 3660-3664.

Janet, C.M.; Viswanath, R.P. Large scale synthesis of CdS nanorods and its utilization in photo-catalytic H_2 production. Nanotechnology 17 (2006): 5271-5277.

Kalyanasundaram, K., Borgarello, E., Duonghong, D., and Gratzel, M. Dynamics of light-induced water cleavage in colloidal systems. Angew. Chem., Int. Ed. Engl. 20 (1981): 987.

Kaneco, S.; Rahman, M.A.; Suzuki, T.; Katsumata, H.; Ohta, K. Optimization of solar photocatalytic degradation conditions of bisphenol A in water using titanium dioxide. J. Photochem. Photobiol. A: Chem. 163 (2004): 419-424.

Kanki, T.; Hamasaki, S.; Sano, N.; Toyoda, A.; Hirano, K. Water purification in a fluidized bed photocatalytic reactor using TiO_2-coated ceramic particles Chem. Eng. J. 108 (2005): 155-160.

Karakitsou, K. E. and Verykios, X. E. Effects of Altervalent Cation Doping of TiO_2 on Its Performance as a Photocatalyst for Water Cleavage. J . Phys. Chem. 97 (1993): 1184-1189.

Kasuga, T.; Hiramatsu, M.; Hoson, A.; Sekino, T.; Niihara, K. Formation of Titanium Oxide Nanotube. Langmuir 14 (1998): 3160-3163.

Kasuga, T.; Hiramatsu, M; Hoson, A.; Sekino, T.; Niihara, K. Titania Nanotubes Prepared by Chemical Processing. Adv. Mater. 11 (1999): 1307-1311.

Keesmann, I. Hydrothermal Synthesis of Brookite. Z. Anorg. Allg. Chem. 346 (1966): 30-43.

Khan, M.; Chatterjee, D.; Krishnaratnam, M.; Bala, M. Photosensitized reduction of N_2 by $RuII(bipy)^{32+}$ adsorbed on the surface of $Pt/TiO_2/RuO_2$ semiconductor

particulate system containing RuIII-EDTA complex and L-ascorbic acid. J. Mol. Catal. 72 (1992): 13-18.

Kim, G.S.; Seo, H.K.; Godble, V.P.; Kim, Y.S.; Yang, O.B.; Shin, H.S. Electrophoretic deposition of titanate nanotubes from commercial titania nanoparticles: Application to dye-sensitized solar cells. Electrochem. Commu. 8 (2006): 961–966.

Lachheb, H.; Eric, P.; Houas, A.; Ksibi, M.; Elaloui, E.; Guillard, C.; Herrmann, J.M. Photocatalytic degradation of various types of dyes (alizarin S, crocein orangeG, methyl red, Congo red and methylene blue) in water by UV-irradiated titania. Appl. Catal. B: Environ. 39 (2002): 75.

Leng, W.H.; Zhang, Z.; Zhang, J.Q. Photoelectrocatalytic degradation of aniline over rutile TiO_2/Ti electrode thermally formed at 600 ^{o}C. J. Molec. Catal. A: Chem. 206 (2003): 239-252.

Lim, S.H.; Juo, J.; Zhong, Z.; Ji W.; Lin, J. Room-Temperature Hydrogen Uptake by TiO2 Nanotubes. Inorg. Chem. 44 (2005): 4124-4126.

Liu, B.J.; Torimoto, T.; Yoneyama, H.; Photocatalytic reduction of CO, using surface-modified CdS photocatalysts in organic solvents. J. Photoch. Photobio. A 113 (1998): 93-97.

Liu, K.; Zhou, W.; Shi, K.; Li, L.; Zhang, L.; Zhang, M.; Fu, H. Influence of calcination temperatures on the photocatalytic activity and photo-induced hydrophilicity of wormhole-like mesoporous TiO_2. Nanotechnology 17 (2006): 1363-1369.

Ma, R.; Fukuda, K.; Sasaki, T.; Osada, M.; Bando, Y. Structural Features of Titanate Nanotubes/Nanobelts Revealed by Raman, X-ray Absorption Fine Structure and Electron Diffraction Characterizations. J. Phys. Chem. B 109 (2005): 6210-6214.

Ma, Y.; Lin, Y.; Xiao, X.; Zhou, X.; Li, X. Sonication–hydrothermal combination technique for the synthesis of titanate nanotubes from commercially available precursors. Mater. Res. Bull. 41 (2006): 237-243.

Meng, X.; Wang, D.; Liu, J.; Shu-yuan Zhang

Nader, A.M. Performance of advanced methods for treatment of wastewater: UV/TiO_2, RO and UF. Chem. Eng. Process. 43 (2004): 935–940.

Nair, M., Luo, Z. H., Heller, A. Rates of photocatalytic oxidation of crude oil on salt water on buoyant, cenosphere-attached titanium dioxide. Ind. Eng. Chem. Res. 32 (1993): 2318-2323.

Nonami, T.; Hase, H.; Funakoshi, K. Apatite-coated titanium dioxide photocatalyst for air purification. Catal. Today 96 (2004): 113–118.

Ogihara, T.; Nakajima, H.; Yanagawa, T.; Ogata, N.; Yoshida, K.; Matsushita, N. Preparation of Monodisperse, Spherical Alumina Powders from Alkoxides. J. Ceram. Soc. 74, 9 (1991): 2263-2269.

Oh, S.; Jin, S. Titanium oxide nanotubes with controlled morphology for enhanced bone growth. Mater. Sci. Eng. C 26 (2006): 1301 – 1306.

Poudel, B.; Wang, W.Z.; Dames, C.; Huang, J.Y.; Kunwar, S.; Wang, D.Z.; Banerjee, D.; Chen, G.; Ren, Z.F. Formation of crystallized titania nanotubes and their transformation into nanowires. Nanotechnology 16 (2005): 1935-1940.

Qamar, M.; Saquib, M.; Muneer, M. Photocatalytic degradation of two selected dye derivatives, chromotrope 2B and amino black 10B, in aqueous suspensions of titanium dioxide. Dyes and Pigments 65 (2005): 1-9.

Randorn, C., Wongnawa, S., and Boonsin, P. Bleaching of Methylene Blue by Hydrated Titanium Dioxide. ScienceAsia 30 (2004): 149-156.

Rohe, B.; Veeman, W.S.; Tausch, M. Synthesis and photocatalytic activity of silane-coated and UV-modified nanoscale zinc oxide. Nanotechnology 17 (2006): 277-282.

Rothenberger, G., Moser, J., Gratzel, M., Serpone, N., and Sharma, D. K. Charge carrier trapping and recombination dynamics in small semiconductor particles. J. Am. Chem. SOC. 107 (1985): 8054.

Sanchez, E.; Lopez, T. Effect of the preparation method on the band gap of titania and platinum-titania sol-gel materials. Materials Letters 25 (1995): 271-275.

Schiavello. M. Some working principles of heterogeneous photocatalysis by semiconductors. Electrochim. Acta. 38 (1993): 11-14.

Seo, D.S.; Lee, J.K.; Kim, H. Preparation of nanotube-shaped TiO_2 powder J. Cryst. Growth 229 (2001): 428-432.

Sjogren, J. C., Sierka, R. A. Inactivation of Phage MS2 by Iron-Aided Titanium Dioxide Photocatalysis. Appl. Environ. Microbiol. 60 (1994): 344-347.

Sun, X.; Li, Y. Synthesis and Characterization of Ion-Exchangeable Titanate Nanotubes. Chem. Eur. J. 9 (2003): 2229-2238.

Suzuki, K. In Photocatalytic Purification and Treatment of Waterand Air. Elsevier: Amsterdam, 1993.

Suzuki, Y.; Yoshikawa, S. Synthesis and thermal analyses of TiO_2-derived nanotubes prepared by the hydrothermal method. J. Mater. Res. 19 (2004): 982-985.

Swarnalatha, B.; Anjaneyulu, Y. Studies on the heterogeneous photocatalytic oxidation of 2,6-dinitrophenol in aqueous TiO_2 suspension. J. Molec. Catal. A: Chem., 223 (2004): 161-165.

Tanaka, K.; Calanag, R.C.R.; Hisanaga, T. Photocatalyzed degradation of lignin on TiO_2. J. Molec. Catal. A: Chemical 138 (1999): 287-294.

Thorne, A.; Kruth, A.; Tunstall, D.; Irvine, T.S.J.; Zhou, W. Formation, Structure, and Stability of Titanate Nanotubes and Their Proton Conductivity. J. Phys. Chem. B 109 (2005): 5439-5444.

Tseng, Y.H.; Kuo, C.S.; Huang, C.H.; Li, Y.Y.; Chou, P.W.; Cheng, C.L.; Wong, M.S. Visible-light-responsive nano-TiO_2 with mixed crystal lattice and its photocatalytic activity. Nanotechnology 17 (2006): 2490-2497.

Viriya-empikul, N.; Sano, N.; Charinpanitkul, T.; Kikuchi, T.; Tanthapanichakoon, W. A step towards length control of titanate nanotubes using hydrothermal reaction with sonication pretreatment. Nanotechnology 19 (2008): 035601.

Wang, Y.Q.; Hu, G.Q.; Duan, X.F.; Sun, H.L.; Xue, Q.K. Microstructure and formation mechanism of titanium dioxide nanotubes. Chem. Phys. Lett. 365 (2002): 427-431.

Weng, L.Q.; Song, S.H.; Hodgson, S.; Baker, A.; Yu, J. Synthesis and characterisation of nanotubular titanates and titania. J. Euro. Ceramic Soc. 26 (2006): 1405-1409.

Xu, J.C.; Lu, M.; Guo, X.Y.; Li, H.L. Zinc ions surface-doped titanium dioxide nanotubes and its photocatalysis activity for degradation of methyl orange in water. J. Molecu. Catal. A: Chem. 226 (2005): 123–127.

Xu, N., Shi, Z., Fan, Y., Dong, J., Shi, J., and Hu, Z.-C. M. Effects of Particle Size of TiO2 on Photocatalytic Degradation of Methylene Blue in Aqueous Suspensions. Ind. Eng. Chem. Res. 38 (1999): 373-379.

Yan, Y.; Qiu, X.; Wang, H.; Li, L.; Fu, X.; Wu, L.; Li, G. Synthesis of titanate/anatase composites with highly photocatalytic decolorization of dye under visible light irradiation. J. Alloys and Compounds xxx (2007) xxx–xxx.

Yang, J.; Jin, Z.; Wang, X.; Li, W.; Zhang, J.; Zhang, S.; Guo, X.; Zhang, Z. Study on composition, structure and formation process of nanotube $Na_2Ti_2O_4(OH)_2$ Dalton Trans. 20 (2003) 3898-3901.

Yuan, Z.Y.; Su, B.L. Titanium oxide nanotubes, nanofibers and nanowires. Colloid Surface A 241 (2004): 173-183.

Zhang, L.; Kanki, T.; Sano, N.; Toyoda, A. Photocatalytic degradation of organic compounds in aqueous solution by a TiO_2-coated rotating-drum reactor using solar light. Solar Energy 70 (2001): 331-337.

Zhang, L., Kanki, T., Sano, N., and Toyoda, A. Development of TiO_2 photocatalyst reaction for water purification. Sepa. Puri. Tech. 31 (2003): 105-110.

Zhang, S.; Peng, L.M.; Chen, Q.; Du, G.H.; Dawson, G.; Zhou, W.Z. Formation Mechanism of $H_2Ti_3O_7$ Nanotubes. Phys. Rev. Lett. 91 (2003): 256103.

Zhao, H.; Xu, S.; Zhong, J.; Bao, X. Kinetic study on the photodegradation of pyridine in TiO_2 suspension systems. Catal. Today 93-95 (2004): 857-861.

Zhu, H.Y.; Lan, Y.; Gao, X.P.; Ringer, S.P.; Zheng, Z.F.; Song, D.Y.; Zhao, J.C. Phase Transition between Nanostructures of Titanate and Titanium Dioxides via Simple Wet-Chemical Reactions. J. AM. CHEM. SOC. 127 (2005): 6730-6736.
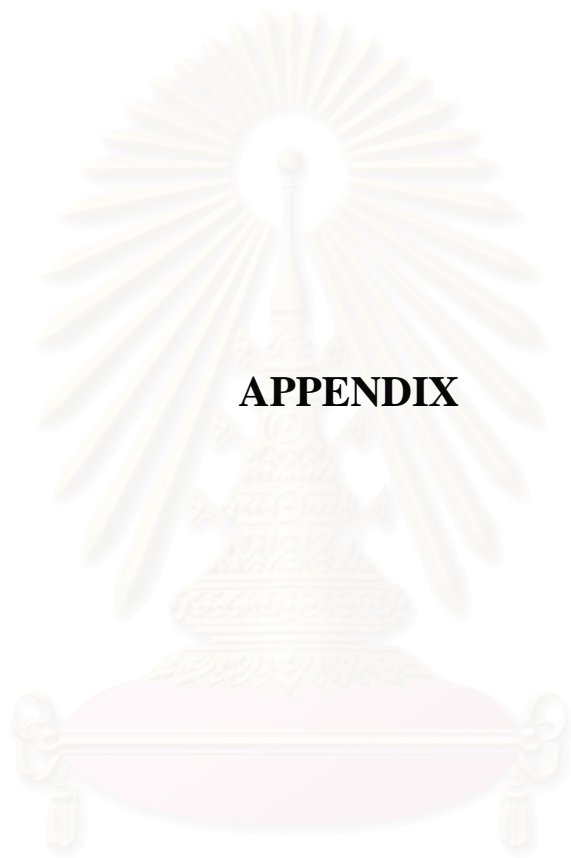
APPENDIX

LIST OF PUBLICATIONS

International Research Paper

1. **N. Viriya-empikul**, N. Sano, T. Charinpanitkul, T. Kikuchi, W. Tanthapanichakoon, "A step towards length control of titanate nanotubes using hydrothermal reaction with sonication pretreatment" **2008**, *Nanotechnology*, Vol. 19, Page 035601.

2. **N. Viriya-empikul**, T. Charinpanitkul, N Sano, N. Thongprachan, A. Soottitantawat, T. Kikuchi, S. Bureekaew and W. Tanthapanichakoon, "Photocatalytic property of titanate nanostructures synthesized by hydrothermal process" submitted 2007.

3. **N. Viriya-empikul**, T. Charinpanitkul, N. Sano, A. Soottitantawat, T. Kikuchi, K. Faungnawakij, and W. Tanthapanichakoon, "Effect of average size of raw titania, reaction temperature and sonication pretreatment on titanate nanotube and nanofiber in hydrothermal reaction" in preparation.

Conference

1. N. Thongprachan, **N. Viriya-empikul**, T. Charinpanitkul, and W. Tanthapanichakoon, "Initial Intrinsic Rates of Photocatalytic Decomposition of Organic Dyes and Compounds Using Titanium Dioxide Nanoparticles" *Proceedings of Thailand Materials Science and Technology Conference 4th*, pp. 218-220. March 31 to April 1, **2006**, Thailand.

2. **N. Viriya–empikul**, N. Sano, T. Charinpanitkul, T. Kikuchi, K. Faungnawakij, W. Tanthapanichakoon, "Effect of Temperature and Sonication Power on Titanate Nanotube Formed in Hydrothermal Reaction" *Proceedings of the 1st Thai–Japanese Scientific Exchange Meeting (TJSE2006)*, November 2–3, **2006**, Osaka, Japan.

3. **N. Viriya-empikul**, T. Charinpanitkul, A. Soottitantawat, T. Kikuchi, N. Sano and W. Tanthapanichakoon, "Characteristics control of titanate nanostructure using hydrothermal reaction method" *Proceedings of The 56th RGJ Seminar Series: CHEMICAL ENGINEERING SCIENCE AND TECHNOLOGY*, September 28, **2007**, Bangkok, Thailand.
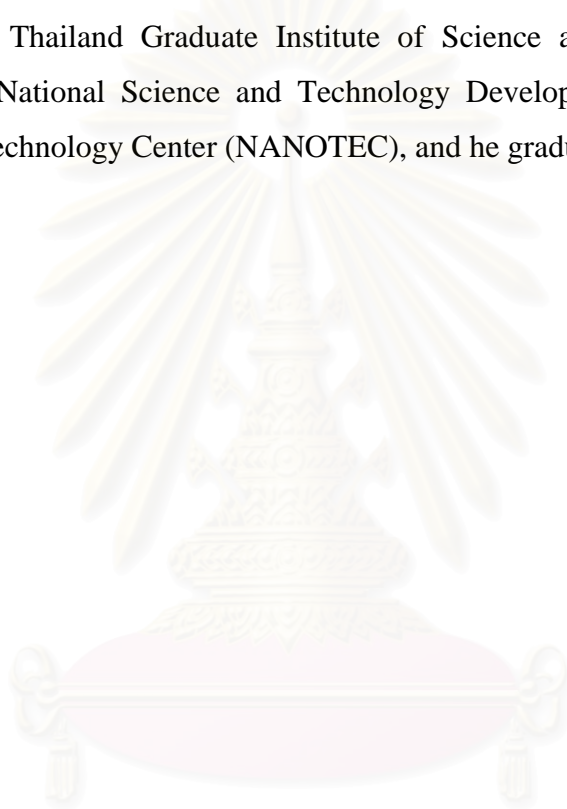
4. T. Muangnapoh, **N. Viriya-empikul**, T. Charinpanitkul and N. Sano, "Effect of pH on stability of gold nanoparticles synthesized by aqueous reaction" *Proceedings of The 14th Regional Symposium on Chemical Engineering (RSCE 2007)*, December 4 – 5, **2007**, Yogyagarta, Indonesia.

5. **N. Viriya-empikul**, T. Charinpanitkul, N. Sano, A. Soottitantawat, T. Kikuchi, K. Faungnawakij, and W. Tanthapanichakoon, "Effect of reaction temperature and sonication pretreatment in the hydrothermal process on the morphology of titanate nanostructure" *submitted to The 20th International Symposium on Chemical Reaction Engineering*, 7 – 10 September **2008**, Kyoto, JAPAN.

VITA

Mr. Nawin Viriya-empikul was born on March 21, 1980 in Bangkok, Thailand. He studied in primary and secondary educations at Assumption College. In 2003, he received the Bachelor Degree of Engineering (Chemical Engineering) from Chulalongkorn University. In 2005, he was awarded the degree of Master of Engineering in Chemical Engineering. After that, he continued to study in Ph.D. program under Thailand Graduate Institute of Science and Technology (TGIST) program from National Science and Technology Development Agency (NSTDA), National Nanotechnology Center (NANOTEC), and he graduated in 2008.